Published in final edited form as:
Mol Microbiol. 2010 June 1; 76(6): 1358–1375. doi:10.1111/j.1365-2958.2010.07165.x.

Characterization of a novel organelle in *Toxoplasma gondii* with similar composition and function to the plant vacuole

Kildare Miranda[1,2,*], **Douglas A. Pace**[1,*], **Roxana Cintron**[1], **Juliany C.F. Rodrigues**[1,2], **Jianmin Fang**[1], **Alyssa Smith**[1], **Peter Rohloff**[1], **Elvis Coelho**[2], **Felix de Haas**[3], **Wanderley de Souza**[2], **Isabelle Coppens**[4], **L. David Sibley**[5], and **Silvia N. J. Moreno**[1,#]

[1]Center for Tropical and Emerging Global Diseases and Department of Cellular Biology, University of Georgia, Athens, GA 30602 [2]Instituto de Biofisica Carlos Chagas Filho, Universidade Federal do Rio de Janeiro, Rio de Janeiro 21941, Brazil [3]FEI Nanoport, Eindhoven, The Netherlands [4]Department of Molecular Microbiology and Immunology, Johns Hopkins University Bloomberg School of Public Health, Baltimore, MD 21205 [5]Department of Molecular Microbiology, Washington University School of Medicine, St. Louis, MO 63110

Abstract

Toxoplasma gondii belongs to the phylum Apicomplexa and is an important cause of congenital disease and infection in immunocompromised patients. Like most apicomplexans, *Toxoplasma gondii* possesses several plant-like features, such as the chloroplast-like organelle, the apicoplast. We describe and characterize a novel organelle in *T. gondii* tachyzoites, which is visible by light microscopy, and possesses a broad similarity to the plant vacuole. Electron tomography shows the interaction of this vacuole with other organelles. The presence of a plant-like vacuolar proton pyrophosphatase (TgVP1), a vacuolar proton ATPase, a cathepsin L-like protease (TgCPL), an aquaporin (TgAQP1), as well as Ca^{2+}/H^{+} and Na^{+}/H^{+} exchange activities, supports similarity to the plant vacuole. Biochemical characterization of TgVP1 in enriched fractions shows a functional similarity to the respective plant enzyme. The organelle is a Ca^{2+} store and appears to have protective effects against salt stress potentially linked to its sodium transport activity. In intracellular parasites, the organelle fragments, with some markers co-localizing with the late endosomal marker, Rab7, suggesting its involvement with the endocytic pathway. Studies on the characterization of this novel organelle will be relevant to the identification of novel targets for chemotherapy against *T. gondii* and other apicomplexan parasites as well.

Introduction

Toxoplasma gondii is a protist parasite that causes widespread infection in humans and has been recognized as a major opportunistic pathogen of immunocompromised patients. Additionally, first time infection with *T. gondii* of pregnant women poses a significant risk to the developing fetus. As a member of the phylum Apicomplexa, *T. gondii* possesses a distinct apical complex consisting of different types of secretory organelles, such as micronemes, dense granules and rhoptries, these latter organelles being acidic (Shaw *et al.*,

[#]To whom correspondence should be addressed: Center for Tropical and Emerging Global Disease and Department of Cellular Biology, 350A Paul D. Coverdell Center, University of Georgia, Athens, GA 30602. Tel.: 706-542-4736; Fax: 706-542-9493; smoreno@cb.uga.edu.
[*]Both authors contributed equally

The name "Plant-Like Vacuole" or PLV was a recommendation of the participants of the 10th International Congress on Toxoplasmosis, in Kerkrade, the Netherlands, June 19–23, 2009.

1998, Dubremetz, 2007). *T. gondii* also contains acidocalcisomes, which are rich in calcium, pyrophosphate, and polyphosphate and are acidified by a membrane-bound vacuolar proton pyrophosphatase (V-H^+-PPase, or TgVP1) (Drozdowicz *et al.*, 2003, Luo *et al.*, 2001). In *T. gondii*, V-H^+-PPase was found also in a large vacuolar compartment of tachyzoites that undergoes dynamic changes during invasion of host cells (Drozdowicz et al., 2003). An association of the V-H^+-PPase with the endosomal/lysosomal pathway was proposed because the enzyme was found to label an endosome-associated compartment (`VP1 compartment') of the secretory pathway. This VP1 positive compartment accumulates microneme protein 2 (MIC2) when the propeptide of the non-anchored microneme protein 2 associated protein (M2AP) is deleted (Harper *et al.*, 2006).

Large vacuolar compartments have been frequently observed in *T. gondii*. Interestingly, the protease cathepsin B localizes to a “large endosomal vacuole” in tachyzoites, distinct from the rhoptries, the primary location of this protease (Que *et al.*, 2002). TgRab51, an homologue of human Rab5, was observed to partially co-localize with TgVP1 (Harper et al., 2006) in similarly described “large lucent vacuoles” that appear “empty” (Robibaro *et al.*, 2002). In addition, FITC-labeled heparin was observed in large “round vesicles” spanning several optical sections of the tachyzoites “sometimes collectively occupying more than 50% of the parasite” (Gross *et al.*, 1993, Botero-Kleiven *et al.*, 2001). These `large vacuoles' have been referred to as pre-rhoptries or forming rhoptries (Robibaro et al., 2002) but a true link with the rhoptry compartment has never been established. In fact, the absence of specific markers has precluded the identification of these large vacuoles as lysosomes, late endosomes, or lysosome-related organelles.

Although disputed (Hunter *et al.*, 2007, Olbrich *et al.*, 2007), there is experimental evidence indicating the presence of two functionally distinct vacuoles in plant cells: a lytic vacuole and a protein-storage vacuole (PSV) (Paris *et al.*, 1996, Jiang *et al.*, 2002). These vacuoles are served by separate vesicular pathways from the Golgi: clathrin-coated vesicles for the lytic vacuole and dense vesicles for the PSV (Paris et al., 1996). Plant lytic vacuoles contain hydrolytic enzymes and function as digestive organelles similar to lysosomes in animal cells (Boller & Kende, 1979). All plant vacuoles contain the vacuolar H^+-ATPase, the V-H^+-PPase and Tonoplast Intrinsic Proteins (TIP)-like aquaporins (Martinoia *et al.*, 2007).

We describe a novel organelle in *T. gondii*, with broad similarities to the plant vacuole that contains transporters usually found in the plant vacuole membrane (tonoplast). In addition, this novel organelle appears to have homeostatic and calcium storage functions in the extracellular stage of the parasite. The relevance of this organelle in *T. gondii* extracellular parasites is discussed in relation to the known functions of the plant vacuole.

Results

A Large Vacuole in Extracellular Tachyzoites Labels with Antibodies Against a Vacuolar-H^+-pyrophosphatase (TgVP1), a cathepsin L (TgCPL) and an aquaporin (TgAQP1)

All plant vacuoles contain the V-H^+-pyrophosphatase (Rea & Poole, 1986), an enzyme that was originally described in *Rhodospirillum rubrum* (Baltscheffsky & von Stedingk, 1966, Moyle *et al.*, 1972), and more recently in acidocalcisomes of several microorganisms (Scott *et al.*, 1998, Docampo *et al.*, 2005), including *T. gondii* (Rodrigues *et al.*, 2000). In order to characterize and study the localization of this enzyme in *T. gondii* we produced antibodies against two distinct peptides in the sequence of the *T. gondii* V-H^+-PPase (TgVP1). Immunofluorescence analysis (IFA) of extracellular tachyzoites with one of these antibodies shows labeling of a large vacuolar structure also clearly observable by differential interference contrast (DIC) microscopy (Fig. 1A and 1B). This enzyme was previously localized to the acidocalcisomes (Rodrigues et al., 2000) and vesicles labeled with the

antibody are observed in all preparations with both antibodies (see Figs. 1B and S1A, *arrows*). Partial co-localization of both antibodies is shown in supplementary Fig. S1A. The specificity of these antibodies was further confirmed by comparing their localization in cells expressing an epitope-tagged version of TgVP1 (Fig. S1B). Western blot analysis of tachyzoite total lysates from RH (wild type strain) and TgVP1-tagged overexpressing parasites also confirmed antibody specificity (Fig. S1C). A band of 80 kDa was detected in cell overexpressing the myc-tagged protein using the anti-myc antibody (Fig. S1C, lane 1) and a second band of 72 kDa, corresponding to the endogenous protein, was detected in total lysates using the anti-TgVP1 antibody (Fig. S1C, lane 3). A size discrepancy between the expected (~89 kDa) and the observed molecular mass has been reported for the V-H^+-PPases of plants (Sarafian *et al.*, 1992, Kim *et al.*, 1994) and trypanosomatids (Hill *et al.*, 2000, Lemercier *et al.*, 2002). It could be attributed either to the anomalous migration of hydrophobic proteins on SDS gels (Maddy, 1976) or to partial degradation. We also show that this large vacuolar compartment labels with anti-TgVP1 by immunoelectron microscopy (IEM) (Fig. 1C, *right panel*). Fig. 1C, *left panel*, shows labeling of a smaller vacuole of the size of an acidocalcisome (about 200 nm) (Luo et al., 2001).

A large vacuolar compartment was also observed in sectioned tachyzoites by transmission electron microscopy (Figs. 2A–C), or by electron tomography (Fig. 2D). This large compartment contained single-membrane-bounded vesicles of diverse size and appearance and was occupied by a less electron dense material than that present in the cytosol (Fig. 2A–C). Some of these vesicles were more electron-lucent and contained very electron-dense material (Fig. 2B, *inset*), as is typical of acidocalcisomes (Docampo et al., 2005). In some cases it was possible to observe typical acidocalcisomes (empty vacuoles containing electron-dense material) in physical contact with this compartment appearing to fuse and even internalize (Fig. 2B–D, *arrow in D*).

Plant lytic vacuoles are characterized by a high content of hydrolytic enzymes, such as proteases, and it has been proposed that amino acid recycling by protein degradation is a major function of the plant vacuole (Muntz, 2007). A cathepsin L-like enzyme (TgCPL) with homology to the previously described vacuolar aleurain from barley (Rogers *et al.*, 1985) has been shown to localize to ultrastructural empty vesicles in *T. gondii* (Huang *et al.*, 2009) (see also (Larson *et al.*, 2009)). We investigated the potential co-localization of TgCPL with TgVP1. As shown in Fig. 3A, TgVP1 and TgCPL show co-localization to the same organelle with TgCPL occupying the interior of a large vacuole while antibodies against TgVP1 labeled its membrane (Movie S1 shows that both markers are in the same compartment). In other cells TgCPL gave a strong reaction in the periphery of the vacuole (see for example Fig. 3B, *TgCPL* and *merge*). This is possible because the propeptide of TgCPL has a transmembrane domain and could be inserted in the membrane. It is possible that the two localizations could represent different stages of maturation of the enzyme, at first membrane-associated and then cleaved to be in the lumen. The accompanying article by Parussini et al. shows in detail the biochemical characterization and subcellular distribution of TgCPL.

The co-localization of TgVP1 and TgCPL in the same compartment was also confirmed by IEM (Figs. 3C, and 3D), showing labeling of both the limiting membrane and internal vesicles (Figs. 3C, and 3D, *arrow* in a vesicle in Fig. 3C).

The *T. gondii* aquaporin water-channel, TgAQP1, has a high similarity to the plant aquaporins known as TIPs, which are found in lytic plant vacuoles (Pavlovic-Djuranovic *et al.*, 2003, Zeuthen *et al.*, 2006). In addition, a motif analysis of representative proteins from the Major Intrinsic Protein (MIP) family of aquaporins supports the close relationship between TgAQP1 and plant gamma-TIPs (see Supplementary Fig. 2). Because the

localization of TgAQP1 has not been reported, we prepared a polyclonal antibody against a C-terminal peptide (LGYVGTHAYHNPVPLRFLNFRGL) of the *TgAQP1* gene. Antibody specificity of anti-TgAQP1 was compared by immunofluorescence and western blot analyses in cells overexpressing an epitope-tagged version of TgAQP1 (Fig. S3). The anti-TgAQP1 antibody did not show a clear and defined reaction when used with wild type parasites. This could be due to the low level of expression of the channel. In this regard, it should be mentioned that some pumps and transporters are found in very low numbers in small vesicles although they are functional. For example, it has been calculated that only one vacuolar H^+-ATPase pump is present per synaptic vesicle (Takamori *et al.*, 2006). However, there is transcript and proteomic information in the Toxoplasma database (ToxoDB) that indicates the expression of this gene in tachyzoites. TgAQP1 detection by antibodies against TgAQP1 and the epitope marker (c-myc) showed a similar discrete localization to a large vacuolar structure in extracellular tachyzoites (data not shown). This localization was consistently observed in a large number of cells (Figs. 4 and S3B and S3C) from multiple IFA preparations. Further analysis using TgAQP1 overexpressing cells and the affinity purified antibody for TgAQP1 showed that the *T. gondii* aquaporin co-localized with both TgCPL (Fig. 4B) and TgVP1 (Fig. 4C) at the site of a large vacuolar structure as visualized by DIC microscopy. Interestingly, the interaction between TgVP1 and TgAQP1 was sometimes complex and involved varying levels of localization to different vacuole compartments that were in physical contact (i.e., budding or fusing) (Fig. S3E–H, and Movie S2). These instances suggest a dynamic relationship between the vacuoles where these markers are present (Fig. 4C and Movie S2, see smaller vacuoles labeled with both TgAQP1 and TgVP1). The affinity-purified antibody against TgAQP1 showed a reaction against a protein of the expected size of 27 kDa by western blot analysis of *T. gondii* lysates of two clones overexpressing TgAQP1 (Fig. S3D, *lanes 1* and *2*). The clones overexpressing the TgAQP1 gene with a triple myc tag showed a reaction with the antibody at 32 kDa (Fig. S3D, *lanes 3* and *4*). No reaction was detected with preimmune serum (not shown).

Our data demonstrates the consistent presence of a large vacuolar compartment in *T. gondii* extracellular tachyzoites. This structure contains a hydrolytic cathepsin L-like protease (TgCPL) as well as a proton pump commonly found in plant vacuoles (TgVP1), thereby suggesting a lytic function to this organelle (see also Parussini et al., accompanying article). Furthermore, the limiting membrane of this structure contains an aquaporin water channel with specific similarities to the plant-γ-TIP aquaporins (TgAQP1). We will refer to this organelle as the Plant-like Vacuole or PLV.

Interaction of the PLV with other Vacuoles

Based on the electron microscopy in Fig. 2 it is evident that the PLV interacts with other vesicles, some of them appearing to be acidocalcisomes (see inset in Fig. 2B). The structural details of the two-dimensional organization of the PLV in these thin sections reveal its approximate size, preferential location in the cell and multi-vesicular nature. However, a general perspective of the organelle as a whole, its interaction with other cell compartments and its substructure at high resolution is better attained with the use of three-dimensional electron microscopy using electron tomography. This analysis revealed in more detail the multivesicular nature of the organelle, presenting vesicles of different sizes and varying levels of interaction with the PLV (i.e., vesicles inside, outside, or in contact with the PLV membrane) (Fig. 2D–G and supplementary movie 3). These results suggest that the PLV is a highly dynamic feature of the cellular architecture of extracellular tachyzoites.

Functional analysis of the PLV

Characterization of TgVP1 Activity in PLV-enriched Fractions—The presence of a vacuolar proton pyrophosphatase (TgVP1) indicates a significant role of the enzyme in the

overall function of the organelle. In order to functionally characterize the biochemical role of this transporter, we generated a tachyzoite RH clone overexpressing the enzyme (see Experimental Procedures) (TgVP1-OE). These cells were used, together with the wild type cells (RH strain), to characterize the V-H^+-PPase activity in PLV-enriched fractions (see below). TgVP1-OE had a higher content of TgVP1 as detected by enzymatic activity (225.08 ± 3.85 and 45.77 ± 4.51 nmol PP_i hydrolyzed min^{-1} × mg of protein in the fraction enriched in PLVs from overexpressing and control tachyzoites, respectively) (Table 1), and immunofluorescence analysis (IFA) (Fig. 1B). V-H^+-PPase activity was assessed measuring AMDP-sensitive production of P_i from pyrophosphate (PP_i) under appropriate conditions (Rodrigues et al., 2000). AMDP is a specific inhibitor of the V-H^+-PPase (Zhen *et al.*, 1994,Rodrigues et al., 2000,Drozdowicz et al., 2003) which we used to discriminate the TgVP1 activity from the activity of other pyrophosphatases. Since the hydrolysis of PP_i releases energy that can be used to pump protons, the activity of TgVP1 could also be measured directly by measuring proton transport using acridine orange (Rodrigues et al., 2000). This proton transport activity was also increased in TgVP1-OE cells (compare slopes of graphs in Fig. 5A and B).

An iodixanol gradient (Rohloff *et al.*, 2004) was used to isolate a fraction enriched in PLVs (Fig. S4A). PLV enrichment was estimated by measuring the AMDP-sensitive V-H^+-PPase activity, and by detection of TgCPL by Western blot analysis. As TgVP1 is not expressed at high levels, isolation of PLVs from wild type RH parasites did not result in fractions with high proton transporting activity (Fig. 5B), prompting the use of TgVP1-OE tachyzoites to characterize the TgVP1 proton translocating activity. Fractionation of TgVP1-OE cells resulted in fraction 1 having the highest specific activity (Table 1) and also the highest percent of activity of TgVP1 (Fig. S4B). In addition, TgCPL was also enriched in fractions 1–3 (Fig. S4B, *bottom panel*). The PLV-enriched fraction did not show enrichment in mitochondrial (cytochrome c reductase activity) or cytosolic (soluble pyrophosphatase activity) markers (Fig. S4C and Table 1), but did show enrichment in acid phosphatase activity, a marker for lysosomes in other cells (de Duve, 2005) (Fig. S4B). A gene (TGME49_004080) encoding a putative acid phosphatase is present in the *T. gondii* database, and peptides of the encoded protein were enriched in Fraction 1 in our proteomic studies (Fig. S4, and S.N.J. Moreno and V. Carruthers, unpublished results).

Proton transport was detected in the enriched PLV fractions from both TgVP1-OE and wild-type tachyzoites (Fig. 5) using acridine orange (Rohloff et al., 2004) indicating the presence of sealed vesicles. Acridine orange accumulates in acidic compartments and the quenching of its fluorescence correlates with the ΔpH (inside acidic). This accumulation is strictly dependent on the presence of PP_i because there was no acridine orange uptake detected in the absence of PP_i (Fig. 5A, *trace -PP_i*) indicating a pyrophosphatase activity. The slope of the tracings correlates with the activity of the enzyme as more protons are actively pumped inside of sealed vesicles. Upon addition of nigericin, a K^+/H^+ ionophore, protons are released from the vesicular compartment in exchange for potassium (see scheme in inset of Fig. 5). Further characterization of PP_i-dependent proton uptake was conducted using different buffers to simulate varying environmental conditions relevant to tachyzoites as well as potential inhibitors of the PPase activity (Figs. 5C,D and S5). Potassium had a stimulatory effect with the maximum proton transport observed at 130 mM KCl (Fig. 5C, *trace a*). Decreasing the amount of KCl from 130 to 65 mM reduced proton pumping activity relative to controls (Fig. 5C, *trace b*), as did replacing KCl with NaCl (Fig. 5C, *trace c*), or replacing KCl and NaCl, with sucrose (Fig. 5C, *trace d*). These results indicate that the TgVP1 is stimulated by K^+, similar to V-H^+-PPases from plant and other protists (Rea & Poole, 1986,Scott et al., 1998,Rodrigues *et al.*, 1999).

Pyrophosphate-induced acidification rate was inhibited in a concentration-dependent manner by the pyrophosphate analogs AMDP and IDP (Fig. 5D, and S5A respectively) and by high concentrations of either NaF or KF (Fig. S5C,D, respectively). Chloroquine, a drug that alkalinizes acidic compartments, was also able to inhibit uptake or stimulate acridine orange efflux depending on the concentration used (Fig. S5B).

It was observed that PLV fractions from both the TgVP1-OE (Fig. 6C) cells and the wild-type tachyzoites (Fig. 6B) had similar ATP-driven acridine orange transport activity (compare Fig. 6B and *trace b* from 6C). However, PLV fractions obtained from TgVP1-OE tachyzoites had much higher PP_i-driven acridine orange uptake (compare the slopes of the tracings of TgVP1-OE and wild-type tachyzoite fractions in Figs 5A and 5B, respectively). The stimulation of proton uptake by ATP indicates the presence of a H^+-ATPase activity which was completely inhibited by 1 μM bafilomycin A_1, (Fig. 6C, *trace a*), a specific inhibitor of V-H^+-ATPases when used at low concentrations (Bowman *et al.*, 1988). This ATP-driven acridine orange uptake was further stimulated by addition of PP_i, at a rate faster than that obtained with ATP alone (Fig. 6C, *trace b*). When the order of additions was reversed, PP_i caused fast acridine orange uptake but addition of ATP did not lead to further accumulation of the dye (Fig. 6C, *trace c*). In both cases, acridine orange was immediately released by addition of nigericin but no additive effects were observed suggesting that the ATP-driven and PP_i-driven proton pumps are located in the same compartment (i.e., the PLV) in this fraction.

Based on the biochemical evidence of ATP-driven proton transport in *T. gondii* PLV fractions (Fig. 6B), we investigated the localization of the V-H^+-ATPase using antibodies against the purified V-H^+-ATPase from *Dictyostelium discoideum* that we previously used to detect localization of this enzyme in *T. gondii* (Moreno *et al.*, 1998). These antibodies react with several subunits of *T. gondii* V-H^+-ATPase, as detected by western blot analysis (Moreno et al., 1998). Interestingly, by IFA these antibodies labeled weakly the plasma membrane and very strongly an intracellular vacuole that at that time we were unable to identify (Moreno et al., 1998). Immunoelectron microscopy revealed labeling of the membrane of the PLV and of internal vesicles (Fig. 6A), a labeling very similar to that obtained with antibodies against TgVP1 (Fig. 3C) and TgCPL (Fig. 3D).

Ion homeostasis and salt stress—Further experiments on enriched PLV fractions showed the presence of additional ion exchange mechanisms. Addition of 80 mM NaCl (Fig. 7A, *trace b*) but not of 80 mM KCl (Fig. 7A, *trace c*) after PP_i-driven acridine orange uptake reached a steady-state level, resulted in acridine orange efflux, suggesting the activity of a Na^+/H^+ exchanger in the PLV fraction (see scheme in inset of Fig. 7A).

We exposed extracellular tachyzoites to high concentrations of NaCl (287 mM final concentration) during short periods of time (30 min), allowed them to infect host cells and evaluated their capacity to form plaques in a fibroblast culture at 9 days after infection. Relative to the number of plaques formed using invasion media, RH cells showed 90% inhibition in the number of plaques formed in the high salt condition (Fig. 7B,C). However, tachyzoites overexpressing the V-H^+-PPase (TgVP1) were significantly more resistant to this treatment, and the number of plaques was only inhibited by 56% under identical treatment (Fig. 7B,C). The number of plaques indicates the number of cells that survive the stress treatment and the results show that TgVP1-OE cells are more resistant to the salt stress. TgVP1 may be facilitating the sequestration of sodium into the PLV and helping the parasite to survive under these extreme conditions. As shown in Fig. 7A sodium transport into the PLV could be coupled to proton transport by the TgVP1.

Calcium storage—Addition of 100 μM $CaCl_2$ to PLV enriched fractions resulted in acridine orange efflux (Fig. 8A, *trace a*), due to calcium being transported into a compartment in exchange for protons (see scheme in inset of A). This result suggests the presence of a Ca^{2+}/H^+ exchanger and indicates that the organelle could be, as is the case in the plant vacuole or the mammalian lysosome, an important acidic calcium store (Patel & Docampo). To test this, we used glycyl-L-phenylalanine-naphthylamide (GPN), which is specifically hydrolyzed in the lysosome of a variety of different cell types by a cathepsin C protease. This results in an increase in osmolarity within the lysosome leading to its swelling and release of stored calcium into the cytosol (Haller *et al.*, 1996,Christensen *et al.*, 2002,Lloyd-Evans *et al.*, 2008). In this regard, our proteomic analysis of the PLV enriched fractions (S.N.J. Moreno and V. Carruthers, unpublished results) revealed the presence of two cathepsin C proteases. In agreement with our hypothesis, addition of GPN to fura-2AM-loaded tachyzoites in the nominal absence of extracellular Ca^{2+} (1 mM extracellular EGTA added) resulted in Ca^{2+} release to the cytosol, which was independent of Ca^{2+} release induced by thapsigargin, a drug that releases Ca^{2+} from the endoplasmic reticulum (Fig. 8C, *trace a*, *two independent peaks are observed*, *evidence of two separate pools*) (Moreno & Zhong, 1996). Similar results were observed when the order of additions was reversed (Fig. 8C, *trace b*). GPN also released calcium after nigericin (Fig. 8B, *trace b*) indicating the presence of a distinct acidic calcium pool (acidocalcisomes), which does not contain a cysteine protease. Similar results were obtained when GPN was added first and nigericin was added second (Fig 8B, *trace a*).

Response to environmental stress—$HgCl_2$ is a specific inhibitor of aquaporin water channels (Niemietz & Tyerman, 2002). With the aim of testing the physiological function of the aquaporins, the ability to tolerate toxic levels of $HgCl_2$ was investigated in wild type (RH) and TgAQP1 overexpressing tachyzoites. When RH tachyzoites were incubated in 1 μM $HgCl_2$ for 5 min, the cells became rounded and the PLV occupied a larger proportion of the cellular volume relative to untreated control cells (Fig. 9A, *RH*). In contrast, tachyzoites overexpressing TgAQP1 showed a much greater tolerance to this stress. Overexpressing mutants of TgAQP1 were less rounded, maintained their typical size and volume, and the PLV retained its usual shape and size when exposed to 1 μM $HgCl_2$ (Fig. 9A, *Tg-AQP-OE*, compare no treatment with mercury treatment). We performed an analysis of overall shape by quantifying the circularity of extracellular tachyzoites when in the presence or absence of 1 μM $HgCl_2$ (Fig. 9B). The circularity of RH cells increased significantly (i.e., the cells became more rounded), the circularity index changing from 0.63 ± 0.07 (SD) to 0.81 ± 0.09 (SD) when incubated in 1 μM $HgCl_2$ (Fig. 9B). The TgAQP1 overexpressing cells had an average circularity similar to the control values of RH at 0.62 ± 0.09 (SD). However, when exposed to 1 μM $HgCl_2$ the general shape of the parasites remained unchanged with an average circularity of 0.63 ± 0.09 (SD).

The PLV in Intracellular Parasites

During intracellular replication of *T. gondii*, the localization of TgCPL and TgVP1 changed as both took on a punctate distribution and their expression no longer localized to a highly visible (i.e., by DIC microscopy) vacuolar structure (Fig. 10A). Proteomic studies of the PLV-enriched fractions (S.N.J. Moreno, and V. Carruthers, unpublished) resulted in the identification of several Rab (Ras-related proteins in the brain) proteins, among them Rab7. Rab proteins are members of the wider Ras superfamily of GTPases and are essential regulators of membrane trafficking. Rab7 is usually associated with late endosomes and lysosomes where it regulates membrane fusion (Stenmark & Olkkonen, 2001). We over-expressed an hemaglutinin (HA) epitope-tagged TgRab7 in *T. gondii* tachyzoites and found that it localizes to a compartment that contains vesicles that label with anti-TgVP1 in intracellular parasites (Fig. 10B). TgRab7 was specifically observed in these vacuoles while

TgVP1 was also observed in other parts of the cells (acidocalcisomes and/or other vacuolar compartments). During intracellular replication the circular profile of the PLV became diminished and the majority of the TgVP1 signal was localized in a post-Golgi compartment as shown by the relative location of the Golgi marker TgGRASP55 (Fig. 10C). Under our experimental conditions, we did not observe co-localization between anti-TgCPL and TgRab7 labeled with anti-HA (not shown). These results suggest that intracellular parasites may not have PLVs and the compartment labeled with Rab7 and TgVP1 corresponds to the previously described "VP1 compartment" (Harper et al., 2006) which would be a pre-PLV compartment with characteristics of a late endosome. This compartment may then form part of the PLV during the transition from intracellular to extracellular parasites. For instance, parasites in 1-cell parasitophorous vacuoles retain a visible PLV showing clear localization of TgVP1, TgCPL and TgAQP1 (Figs. 10D, and S6, *one parasite panels*). However, from the 2-cell stage onward, the structure of the PLV is no longer noticeable by DIC or antibody labeling of these markers. This fragmentation (Larson et al., 2009) and apparent loss of the PLV results in anti-TgVP1 and anti-TgAQP1 only partially co-localizing with anti-TgCPL (Fig. 10A). Parussini et al. describe in detail in the accompanying article the PLV fragmentation during daughter cell formation.

The PLV Appears in Recently Egressed Extracellular Parasites

Due to the observed fragmentation of the PLV during intracellular replication, further analysis was conducted on extracellular tachyzoites to better understand its occurrence during the entire extracellular stage. Intracellular tachyzoites from semisynchronized cultures were released by scrapping off the host monolayer and passage through a syringe needle. These parasites were immediately collected and incubated under two different conditions (BAG vs. IM, see description under Experimental Procedures and legend to Fig. 11) for 0, 2 and 4 h, during which time the shape of the PLV (closed vs. open) and number of PLV-containing parasites were evaluated (Table 2). Fig. 11 shows the results obtained from one representative experiment. It is noticeable that under the conditions of the extracellular buffer BAG, the parasites show a more open PLV when compared to the same parasites in Invasion Media (IM) (Table 2). Analysis of invading tachyzoites showed that the PLV was localized to the apical end of parasites at the onset of invasion (Fig. 11B *invading tachyzoite*). In this regard, a similar clear vacuole appears in invading tachyzoites in Fig. 5C and accompanying movie of ((Lovett & Sibley, 2003). As described above, once inside the host cell the PLV diminished as replication progressed. The presence of an open (i.e., large and circular) PLV in recently released as well as actively invading parasites indicate that the PLV is a normal aspect of tachyzoite morphology and not an artifact observed in degenerating or aging cells.

Discussion

We report the identification of a previously uncharacterized organelle in tachyzoites of *T. gondii*. This organelle is a large multivesicular structure that possesses similarities to the central vacuoles found in plant cells. Similarities in structure, composition and potential functions prompted us to name this organelle the plant-like vacuole, or PLV. This organelle labels with antibodies against proteins with great similarity to vacuolar plant pumps and channels, such as a K^+-sensitive V-H^+-PPase (TgVP1), and an aquaporin water channel (TgAQP1). It is interesting to note that Drozdowicz et al. (2003) detected the localization of TgVP1 to a large vacuole in invading tachyzotes that we can now identify as the PLV. Sequence analysis has shown that TgAQP1 groups with other coccidian apicomplexan aquaporins such as *Emeria* sp. (Pavlovic-Djuranovic et al., 2003). Interestingly these aquaporins share a plant-like divergence from other aquaporins (e.g., *Plasmodium* sp.) in that the highly conserved arginine residue at the aromatic arginine region of the channel

pore (Ar/R region) has been replaced with a valine residue (Pavlovic-Djuranovic et al., 2003). This substitution is characteristic of Tonoplast Intrinsic Proteins (TIPs) from plants and has a significant function in determining transport capabilities of these channels. Such analyses have been used to infer that apicomplexan aquaporins may have been adopted from different taxonomic sources, with the *Plasmodium* sp. aquaporins deriving from bacterial glycerol facilitators and the *T. gondii* aquaporin originating from a plant TIPs (Pavlovic-Djuranovic et al., 2003). This analysis further supports the plant-like nature of TgAQP1 and of the PLV. In addition, all plant vacuoles contain the V-H^+-PPase supporting the similarity of the PLV to plant vacuoles. Physiological evidence revealed further similarities to plant vacuoles such as the presence of a V-H^+-ATPase, a Na^+/H^+ exchanger, and a Ca^{2+}/H^+ exchanger, and the storage of calcium (Maeshima, 2001, Becker, 2007).

Many proteases reside in the lumen of plant vacuoles and are used for protein degradation to produce amino acids that are recycled for metabolic processes that take place outside the vacuole (Muntz, 2007). Cathepsin L-like proteases (Bethke *et al.*, 1996, Vincent & Brewin, 2000) have been described in a number of plant vacuoles (Boller & Kende, 1979) and our results show the localization of a cathepsin L-like protease (TgCPL) in the PLV. The observation that TgCPL is inside vesicles as well as in the membrane of the PLV is interesting. It is possible that this lytic enzyme has two distinct locations based on the maturation of its propeptide or that it is temporarily compartmentalized to avoid contact with its substrates as is the case in the plant vacuole (Jiang *et al.*, 2001).

Our results show that the PLV is a prominent feature of extracellular tachyzoites and with multiple potential functions as is the case for the plant vacuole in the plant cell. We show evidence for its potential role in the transport of sodium and calcium, calcium storage, and in resistance to environmental stresses, although we cannot rule out that some of the functions attributed to the presence of TgAQP1 and TgVP1 in the PLV could be shared with other organelles in which these proteins are located. Transgenic plants overexpressing the V-H^+-PPase are much more resistant to high concentrations of NaCl than the wild-type strains (Gaxiola *et al.*, 2001). When *T. gondii* tachyzoites egress from the host cell they are exposed to an abrupt change in sodium from the intracellular concentration of 2–5 mM to the extracellular concentration of 100–150 mM. Parasites have to survive under these conditions long enough to find other host cells to invade. Our salt stress experiments combined with Na^+/H^+ exchange activity observed in PLV fractions, strongly suggest that TgVP1 might have a role in the homeostasis of intracellular sodium by helping to sequester it into the PLV.

Our analysis of semisynchronized cells shows that the PLV is already present in freshly egressed tachyzoites as well as invading tachyzoites, indicating that the PLV fulfills important physiological functions and is not a consequence of aging parasites. We find a significant difference in the appearance and size of the PLV that is related to the conditions of the extracellular media. Extracellular tachyzoites incubated in basic extracellular media (BAG) show a more prominently open PLV. Parasites collected in Ringer buffer also gave a similar result (not shown). When parasites were prepared and incubated in a media containing significantly less NaCl (IM, 50% less NaCl) the appearance of the PLV was diminished and collapsed. It is possible that ionic composition plays a large role in the morphology of the PLV with NaCl being at least one important determinant of its state. Future work analyzing in more detail the specific component(s) that produces these changes in the morphology of the PLV will help clarify this phenomenon.

During intracellular replication, the co-localization of TgVP1 and TgCPL is not clearly evident or consistent. Instead, TgVP1 co-localizes with TgRab7 to a vacuolar compartment, potentially a late endosome. This is interesting because it might shed light into the

generation of this organelle as the parasites leave the host cell and prepare to confront the external environment. It is possible that the PLV is formed through the fusion of a late endosome (because of its labeling with Rab7) containing TgVP1 (the "VP1 compartment" described by (Harper et al., 2006)) and TgAQP1 with lysosome-like vacuoles containing TgCPL. This structure is then maintained in extracellular tachyzoites until after invasion of a new host cell (See our proposed model in Fig. S7). We propose that this VP1 compartment functions as a pre-PLV compartment in intracellular parasites, which fuses with other vesicles to form the PLV in extracellular parasites.

In this work we have also characterized for the first time the proton pumping activity of *T. gondii* V-H^+-PPase (TgVP1). Pyrophosphate-driven proton transport was inhibited by the PP_i analogs IDP and AMDP and was stimulated by K^+ ions. In this regard, AMDP and other PP_i analogs have been shown to inhibit *T. gondii* growth (Rodrigues et al., 2000, Drozdowicz et al., 2003). In plants, the V-H^+-PPase and the V-H^+-ATPase are located in the same membrane (Rea *et al.*, 1992) and in our enriched PLV fractions, we observed that there is no additive acidification induced by ATP or PP_i suggesting that both pumps are present in the same vacuole.

Plant lytic vacuoles, which are acidic and rich in hydrolases are considered as equivalent to the animal lysosome and are recognized by the presence of γ-TIP (Becker, 2007). Sequence analysis of TgAQP1 demonstrated its similarity with plant γ-TIPs (Fig. S2), which are specific of the plant lytic vacuole (Martinoia et al., 2007). We used the major intrinsic protein database (MIPDB) as a reference to retrieve representative protein sequences from each MIP subfamily (there are ~8 MIP subfamilies, plants contain three subfamilies: PIPs, TIPs and NIPs). We identified a total of five conserved motif regions in the TgAQP1 sequence (Figs. S2A and B). Of these five motifs, four were exclusively associated with the plant γ-TIP family (Fig. S2A, motifs 1–4, *green*). The fifth motif belonged to the prokaryotic glycerol facilitator subfamily and is present in several taxonomically divergent taxa (e.g., *Plasmodium* sp., *Neospora* sp., and plants). These results confirm previous sequence analysis showing that TgAQP1 has a high similarity to plant γ-TIPs (Pavlovic-Djuranovic et al., 2003, Zeuthen et al., 2006) and provide further support to the similarity between the *T. gondii* vacuole and the plant lytic vacuole.

Plant cell vacuoles are part of the eukaryotic endomembrane system and exhibit a wide diversity in form and function (Becker, 2007, Marty, 1999). Plants have evolved a large central vacuole to allow them to increase their cell volume without the need to invest in cytoplasm and other organelles (Becker, 2007). Many protists, especially those that live in water, posses contractile vacuoles (CV) involved in osmoregulation as well as other acidic vacuoles like acidocalcisomes for storage of phosphorus and cations. *T. gondii* contains acidocalcisomes and it is possible that it acquired an organelle similar to the one found in plants through convergent evolution. Plant vacuoles are thought to have a division of labor between storage and lytic vacuoles, and a similar situation might be occurring in *T. gondii* tachyzoites. Our characterization of the PLV has also demonstrated that it not only has a high degree of physical interaction with acidocalcisomes but also possesses markers that are common to acidocalcisomes (e.g., TgVP1 and H^+-ATPase). It may be that acidocalcisomes in *T. gondii* have an analogous role as plant storage vacuoles and that the PLV is fulfilling functions in *T. gondii* tachyzoites that are done by lytic vacuoles in plants.

The PLV is a proton sequestering organelle driven by PP_i and ATP and appears to possess several other ion exchange mechanisms. A model showing how these pumps would work in combination with other transporters (*e.g.*, sodium, calcium and other cations) is shown in Fig. 12. Considering the role of the plant vacuole, and based on our findings, the PLV could have an homeostatic function providing protective mechanisms needed by extracellular

tachyzoites to survive in diverse biological environments. Although *T. gondii* is an obligate intracellular parasite, it is still not completely understood how tachyzoites disperse throughout the host organism as they can cross the intestinal epithelium, disseminate into the deep tissues, and actively traverse biological barriers such as the placenta and the blood-brain barriers (Barragan & Sibley, 2003,Tardieux & Menard, 2008). We propose that the PLV plays a critical role in this biological context. The PLV could also provide "turgor pressure" to the parasite to facilitate active egress from the host cell or active penetration into a new host cell in the same way that the plant vacuole provides turgidity. During intracellular replication the pre-PLV compartment may play additional roles involved in the endocytic/exocytic pathways where the sorting of proteins targeted to various organelles necessary for invasion and egress occurs. The accompanying manuscript by Parussini et al. provides evidence for a role of this compartment in the proteolytic maturation of pro-proteins targeted to micronemes. This plant-like organelle has not been described before in any non-plant organism. Its detailed characterization will help in better understanding the adaptive responses of *T. gondii* tachyzoites during the extracellular stage when it has the capability of invading numerous types of host cells. It is quite likely that the PLV is also present in other apicomplexan parasites and further studies will be relevant to the identification of novel targets for chemotherapy against *T. gondii* and other parasites as well.

Experimental Procedures

Parasites

T. gondii tachyzoites (RH strain) were grown in h-Tert human fibroblasts (Farwell *et al.*, 2000) as described before (Moreno & Zhong, 1996). These cells grow in DMEM media containing 1% FBS.

For semisynchronization of cultures, h-Tert cells cultured in 75 cm^2 flasks, were infected with 3.7×10^7 tachyzoites/flask for two hours, extracellular parasites thoroughly washed and the cultures allowed to grow for 35–40 hours. At this time, extracellular parasites were removed by washing with fresh invasion medium (IM) (DMEM containing 20 mM Hepes pH 7.4 with 1% FBS) 3 times and the cultures allowed growth for two more hours in IM. Subsequently, the extracellular tachyzoites were washed off and the intracellular tachyzoites collected in fresh IM by scrapping off the host monolayer and purifying the parasites by filtration through a nucleopore membrane. The isolated tachyzoites were centrifuged and resuspended in IM without serum or Buffer A plus glucose (BAG) (116 mM NaCl, 5.4 mM KCl, 0.8 mM $MgSO_4$, 50 mM Hepes, pH 7.2, 5.5 mM glucose) at a concentration of 5×10^7 tachyzoites/ml, and incubated for two or four hours at 37°C.

For stress experiments involving mercury tolerance, tachyzoites were incubated in BAG with 1 μM $HgCl_2$ for 5 min, fixed with 4% paraformaldehyde and mounted on coverslips. Using Image J software (NIH), circularity measurements (a metric of roundness where 1 equals a perfect circle) were made on 50 randomly chosen cells from each treatment to determine changes in overall cell shape when in the presence or absence of 1 μM $HgCl_2$.

For salt stress experiments freshly egressed tachyzoites were purified and washed in IM, incubated for 15 and 30 min under stress conditions (described in the legend for Fig. 7) and subsequently added to the regular culture medium. For plaque assays confluent monolayers of fibroblasts grown in 6 well plates were infected, in triplicate, with 225 tachyzoites per well. The parasites were allowed to plaque for 9 days, fixed, and stained as described (Roos *et al.*, 1994).

Isolation of PLV-Enriched Fractions

Isolation of PLV-enriched fractions was according to a modification of a method described previously for the isolation of contractile vacuoles from *Trypanosoma cruzi* (Rohloff et al., 2004) (Fig. S4). Tachyzoites (~1–2 × 10^{10} cells) were purified and washed with lysis buffer (125 mM sucrose, 50 mM KCl, 4 mM $MgCl_2$, 0.5 mM EDTA, 20 mM K-Hepes pH 7.2, 5 mM dithiothreitol, protease inhibitors (0.2% v/v), 12 mg/ml DNAse, 12 mg/ml RNAse, and 8 mg/ml nocodazole). The pellet was mixed with 2 × wet weight silicon carbide and grinded for 60 s. This mixture was re-suspended in approximately 40 ml of lysis buffer and the suspension decanted and clarified by three low speed centrifugations. The supernatant was centrifuged at 15,000 *g* for 10 min, and the new supernatant centrifuged at 100,000 *g* for 60 min. The resulting pellet (P3) was homogenized and loaded into the 20% layer of an iodixanol gradient containing 4-ml steps of 15, 20, 25, 30, 34, and 38%. The gradient was centrifuged at 50,000 *g* for 60 min. 15 fractions of 1.8 ml each were collected from the top of the gradient. Fractions 1–3 were the PLV-enriched fractions (Fig. S4).

Antibody Generation and Purification

Guinea pig and rabbit polyclonal antisera were raised against synthetic peptides corresponding to amino acids GLGPEVRSRTDALDA (between transmembrane region 11 and 12) and SGKNEYGMSEDDPRN (between transmembrane region 6 and 7) of the TgVP1 sequence respectively, and affinity purified by Covance Research Products (Berkeley, CA). The antibodies were shown to react with a protein of 72 kDa in subcellular fractions of *T. gondii* (Fig. S1C). No reaction was detected with preimmune serum for either antibody. A peptide (LGYVGTHAYHNPVPLRFLNFRGL) from the C-terminal domain of the TgAQP1 sequence was synthesized by Covance Inc. and used to generate antibodies in rabbit. The affinity-purified antibody showed a reaction against a protein of approx. 27 kDa (Fig. S3D).

Enzyme Assays and Calcium Measurements

Pyrophosphatase activities were assayed by measuring phosphate release using the malachite green assay (Lanzetta *et al.*, 1979). Aminomethylenediphosphonate (AMDP) was used to distinguish between the vacuolar and the soluble activity. Acid phosphatase was assayed by measuring phosphate release from *p*-nitrophenylphosphate (Rodrigues *et al.*, 2002) in acetate buffer pH 5.0.

PP_i- and ATP-driven proton transport in PLV-enriched fractions was measured by changes in the fluorescence of Acridine Orange at excitation and emission wavelengths of 470 and 526 nm, respectively, using a Molecular Devices Microplate Reader. Fractions were incubated in a 200 μl final volume of a solution which is described in the Fig. legends, plus 3 μM Acridine Orange for 3 min prior to the addition of 100 μM PPi or 0.5 mM ATP. Nigericin was used to collapse the membrane potential generated. Each experiment was repeated at least three times with different fractionations, and the figures show representative experiments.

Intracellular calcium measurements were performed using fura-2AM (Invitrogen) as previously described (Moreno & Zhong, 1996).

Overexpression of the TgVP1, TgRab7 and TgAQP1

We isolated tachyzoites that overexpress the vacuolar proton pyrophosphatase by transfecting cells of the RH strain with the plasmid ptubTgVP1-FLAG/sag-CAT (Striepen *et al.*, 1998), which contains the entire coding sequence of the TgVP1 gene (Drozdowicz et al., 2003) (GenBank: AAK38077.1; Toxodb: TGME49_048670). This plasmid was made by replacing the P30 gene with the coding sequence of the TgVP1 in the vector ptubP30-

FLAG/sag-CAT (Luo *et al.*, 2005). Selection was done in the presence of chloramphenicol and one clone was selected for further analysis. TgVP1-OE had a higher content of TgVP1 as detected by western blot (Fig. S1C), proton transport activity (Table 1) and immunofluorescence analyses (Figs. 1A–B, 3A–B).

The entire open reading frame of *TgAQP1* (GenBank: AAP33053.1; Toxodb: TGME49_015450) was amplified by RT-PCR from *T. gondii* cDNA. The forward primer (5'-AGATCT ATGGACCAATTTGTTTTTTCAGGAGGTTC -3') included the *Bgl*II restriction site (*underlined*), which is compatible with the *Bam*HI site in the vector. The reverse primer (5'-CCTAGG GAGCCCCCTGAAGTTCAAGA -3') omitted the stop codon and introduced an *Avr*II restriction site (*underlined*). The PCR product was cloned into the expression vector pDTM3 (provided by Dr. Boris Striepen) between the *Bgl*II/*Avr*II sites, creating a triple-c myc epitope-tagged version of TgAQP1. The created pDTM3AQP-1 recombinant plasmid was confirmed by DNA sequencing. *T. gondii* RH tachyzoites were transfected with 50 μg of plasmid DNA and selected with 1 μM of pyrimethamine. An alternative construct was also made in the same vector but the stop codon of TgAQP1 was not omitted, therefore removing the triple-c myc epitope. For these constructs, AQP1 was detected with the peptide antibody to the C-terminal domain of TgAQP1 (see above).

The entire open reading frame of TgRab7 (GenBank: XP_002367234.1; ToxoDB: TGME49_048880) was amplified by RT-PCR from *T. gondii* cDNA. The forward primer (5'-TCCCCCGGGATGCCGC CCAAGAAGAAGG-3') included the XmaI restriction site (underlined). The reverse primer (5'-CGCG GACGTCTCAGCAGCAGCCGCCG-3') included the stop codon and introduced an AatII restriction site (underlined). The recombinant TgRab7 was cloned into the pCTH expression vector (provided by Dr. Boris Striepen) between the XmaI/AatII sites. The pCTH-TgRab7 recombinant plasmid was confirmed by DNA sequencing. Twenty-five micrograms of recombinant plasmid (pCTH-TgRab7) were used to transfect T. gondii tachyzoites, which were inoculated in 12-well plates containing hTERT fibroblasts grown in coverslips. Parasites were cultured for 16–20 hours and used for IFA analysis.

Fluorescence Microscopy

T. gondii tachyzoites were harvested and washed with BAG or Ringer buffer (155 mM NaCl, 3 mM KCl, 1 mM $MgCl_2$, 3 mM NaH_2PO_4-H_2O, 10 mM Hepes, pH 7.2, 10 mM glucose) and fixed with 4% formaldehyde for 1 h. Immunofluorescence assays were performed as described (Luo et al., 2001) by using primary antibodies at the concentrations indicated in the legends. Secondary antibodies were Alexa 488 and Alexa 546 conjugated anti-rabbit IgG or Alexa 488 and Alexa 568 (1:500 or 1:1000) conjugated anti-mouse (Molecular Probes). Fluorescence images were collected with an Olympus IX-71 inverted fluorescence microscope with Photometrix $CoolSnap_{HQ}$ CCD camera driven by DeltaVision software (Applied Precision, Seattle, WA). Collected images were deconvolved using Softworx deconvolution software (Applied Precision, Seattle, WA). For all images, 15 cycles of enhanced ratio deconvolution were used.

Electron Microscopy

For conventional transmission electron microscopy cells were washed in Buffer A or Ringer buffer, pH 7.2, fixed in 2.5% glutaraldehyde, 4% paraformaldehyde in 0.1 M cacodylic acid buffer, postfixed in 1% OsO_4 plus 0.8% ferrocyanide and 5 mM $CaCl_2$ in 0.1 M cacodylic acid buffer for 30 min, dehydrated in acetone series, and embedded in Polibed 812 epoxide resin. Sections of 70 nm were obtained and stained for 40 min in 5% aqueous uranyl acetate and for 5 min in lead citrate pH 12.0. Observation was made in a Zeiss 900 transmission electron microscope operating at 80 kV.

Electron Tomography

Four hundred nanometer sections of epoxide embedded tachyzoites were obtained, collected in 200 mesh copper grids and stained as above. Tomographic tilt series over a range of 120° (± 60°) by 1° angular increments were collected an in a Tecnai 20 transmission electron microscope (FEI company, Eindhoven, The Netherlands) operating at 200kV. Images were recorded on a bottom mounted Eagle 4K CCD camera. Alignment of the tilt series was performed by cross correlation using the Inspect 3D software package (FEI company). 3D reconstruction was calculated by weighted back projection. Segmentation and generation of a 3D model was calculated using IMOD software (Kremer *et al.*, 1996).

Immunoelectron Microscopy

For single localization studies by cryoimmunoEM, infected cells were fixed in 4% paraformaldehyde/0.05% glutaraldehyde (Polysciences Inc., Warrington, PA) in 100 mM PIPES buffer. Samples were then embedded in 10% gelatin and infiltrated overnight with 2.3 M sucrose/20% polyvinyl pyrrolidone in PIPES at 4°C. Samples were frozen in liquid nitrogen and sectioned with a cryo-ultramicrotome. Sections were probed with purified rabbit anti-TgVP1 antibody (1:100) followed by secondary antibody conjugated to 18 nm colloidal gold, stained with uranyl acetate/methylcellulose, and analyzed by transmission EM.

For double localization studies, extracellular *T. gondii* were washed twice with PBS before fixation in 4% paraformaldehyde (Electron Microscopy Sciences, PA) in 0.25 M HEPES (pH 7.4) for 1 h at room temperature, then in 8% paraformaldehyde in the same buffer overnight at 4°C. Parasites were pelleted in 10% fish skin gelatin and the gelatin-embedded pellets were infiltrated overnight with 2.3 M sucrose at 4°C and frozen in liquid nitrogen. Ultrathin cryosections were incubated in PBS and 1% fish skin gelatin containing anti-TgCPL or TgVP1 antibodies at 1:600 and 1:200 dilutions, respectively, and then exposed to the secondary antibodies that were revealed with protein A-gold conjugates.

Supplementary Material

Refer to Web version on PubMed Central for supplementary material.

Acknowledgments

We thank Melina Galizzi and Cuiying Jiang for excellent technical assistance. We would like to specially thank Drs. Vern Carruthers (University of Michigan) and Fabiola Parussini for sharing unpublished information and reagents, for extensive discussions and critically reading the manuscript. We also would like to thank William Sullivan (University of Indiana) and Boris Striepen (University of Georgia) for *Toxoplasma* expression plasmids. Technical assistance with cryoimmunoEM (Fig. 1C) was provided by Wandy Beatty, Microbiology Imaging Facility (Washington University). We also thank Lia Carolina Medeiros for helping with movie renderization from the tomography data. This work was supported by U.S. National Institutes of Health Grant AI-079625 to S.N.J.M, and AI-034036 to L.D.S. K.M. was supported by a training grant from the Ellison Medical Foundation to the Center for Tropical and Emerging Global Diseases, Fundação Carlos Chagas Filho de Amparo a Pesquisa do Estado do Rio de Janeiro (FAPERJ) and Programa Jovens Pesquisadores CNPq-Brazil. D.A.P. was partially supported by an NIH T32 training grant AI-60546 to the Center for Tropical and Emerging Global Diseases. R.C.was supported in part by NIH research supplement 3R01AI068647-04S1.

References

Baltscheffsky H, von Stedingk LV. Bacterial photophosphorylation in the absence of added nucleotide. A second intermediate stage of energy transfer in light-induced formation of ATP. Biochem Biophys Res Commun 1966;22:722–728. [PubMed: 5944772]

Barragan A, Sibley LD. Migration of Toxoplasma gondii across biological barriers. Trends Microbiol 2003;11:426–430. [PubMed: 13678858]

Becker B. Function and evolution of the vacuolar compartment in green algae and land plants (Viridiplantae). Int Rev Cytol 2007;264:1–24. [PubMed: 17964920]

Bethke PC, Hillmer S, Jones RL. Isolation of Intact Protein Storage Vacuoles from Barley Aleurone (Identification of Aspartic and Cysteine Proteases). Plant Physiol 1996;110:521–529. [PubMed: 12226201]

Boller T, Kende H. Hydrolytic Enzymes in the Central Vacuole of Plant Cells. Plant Physiol 1979;63:1123–1132. [PubMed: 16660869]

Botero-Kleiven S, Fernandez V, Lindh J, Richter-Dahlfors A, von Euler A, Wahlgren M. Receptor-mediated endocytosis in an apicomplexan parasite (Toxoplasma gondii). Exp Parasitol 2001;98:134–144. [PubMed: 11527436]

Bowman EJ, Siebers A, Altendorf K. Bafilomycins: a class of inhibitors of membrane ATPases from microorganisms, animal cells, and plant cells. Proc Natl Acad Sci U S A 1988;85:7972–7976. [PubMed: 2973058]

Christensen KA, Myers JT, Swanson JA. pH-dependent regulation of lysosomal calcium in macrophages. J Cell Sci 2002;115:599–607. [PubMed: 11861766]

de Duve C. The lysosome turns fifty. Nat Cell Biol 2005;7:847–849. [PubMed: 16136179]

Docampo R, de Souza W, Miranda K, Rohloff P, Moreno SN. Acidocalcisomes - conserved from bacteria to man. Nat Rev Microbiol 2005;3:251–261. [PubMed: 15738951]

Drozdowicz YM, Shaw M, Nishi M, Striepen B, Liwinski HA, Roos DS, Rea PA. Isolation and characterization of TgVP1, a type I vacuolar H+-translocating pyrophosphatase from Toxoplasma gondii. The dynamics of its subcellular localization and the cellular effects of a diphosphonate inhibitor. J Biol Chem 2003;278:1075–1085. [PubMed: 12411435]

Dubremetz JF. Rhoptries are major players in Toxoplasma gondii invasion and host cell interaction. Cell Microbiol 2007;9:841–848. [PubMed: 17346309]

Farwell DG, Shera KA, Koop JI, Bonnet GA, Matthews CP, Reuther GW, Coltrera MD, McDougall JK, Klingelhutz AJ. Genetic and epigenetic changes in human epithelial cells immortalized by telomerase. Am J Pathol 2000;156:1537–1547. [PubMed: 10793065]

Gaxiola RA, Li J, Undurraga S, Dang LM, Allen GJ, Alper SL, Fink GR. Drought- and salt-tolerant plants result from overexpression of the AVP1 H+-pump. Proc Natl Acad Sci U S A 2001;98:11444–11449. [PubMed: 11572991]

Gross U, Hambach C, Windeck T, Heesemann J. Toxoplasma gondii: uptake of fetuin and identification of a 15-kDa fetuin-binding protein. Parasitol Res 1993;79:191–194. [PubMed: 7684138]

Haller T, Dietl P, Deetjen P, Volkl H. The lysosomal compartment as intracellular calcium store in MDCK cells: a possible involvement in InsP3-mediated Ca2+ release. Cell Calcium 1996;19:157–165. [PubMed: 8689673]

Harper JM, Huynh MH, Coppens I, Parussini F, Moreno S, Carruthers VB. A cleavable propeptide influences Toxoplasma infection by facilitating the trafficking and secretion of the TgMIC2-M2AP invasion complex. Mol Biol Cell 2006;17:4551–4563. [PubMed: 16914527]

Hill JE, Scott DA, Luo S, Docampo R. Cloning and functional expression of a gene encoding a vacuolar-type proton-translocating pyrophosphatase from Trypanosoma cruzi. Biochem J 2000;351:281–288. [PubMed: 10998372]

Huang R, Que X, Hirata K, Brinen LS, Lee JH, Hansell E, Engel J, Sajid M, Reed S. The cathepsin L of Toxoplasma gondii (TgCPL) and its endogenous macromolecular inhibitor, toxostatin. Mol Biochem Parasitol 2009;164:86–94. [PubMed: 19111576]

Hunter PR, Craddock CP, Di Benedetto S, Roberts LM, Frigerio L. Fluorescent reporter proteins for the tonoplast and the vacuolar lumen identify a single vacuolar compartment in Arabidopsis cells. Plant Physiol 2007;145:1371–1382. [PubMed: 17905861]

Jiang L, Erickson A, Rogers J. Multivesicular bodies: a mechanism to package lytic and storage functions in one organelle? Trends Cell Biol 2002;12:362–367. [PubMed: 12191912]

Jiang L, Phillips TE, Hamm CA, Drozdowicz YM, Rea PA, Maeshima M, Rogers SW, Rogers JC. The protein storage vacuole: a unique compound organelle. J Cell Biol 2001;155:991–1002. [PubMed: 11739409]

Kim Y, Kim EJ, Rea PA. Isolation and characterization of cDNAs encoding the vacuolar H(+)-pyrophosphatase of Beta vulgaris. Plant Physiol 1994;106:375–382. [PubMed: 7972521]

Kremer JR, Mastronarde DN, McIntosh JR. Computer visualization of three-dimensional image data using IMOD. J Struct Biol 1996;116:71–76. [PubMed: 8742726]

Lanzetta PA, Alvarez LJ, Reinach PS, Candia OA. An improved assay for nanomole amounts of inorganic phosphate. Anal Biochem 1979;100:95–97. [PubMed: 161695]

Larson ET, Parussini F, Huynh MH, Giebel JD, Kelley AM, Zhang L, Bogyo M, Merritt EA, Carruthers VB. Toxoplasma gondii cathepsin l is the primary target of the invasion inhibitory compound LHVS. J Biol Chem. 2009

Lemercier G, Dutoya S, Luo S, Ruiz FA, Rodrigues CO, Baltz T, Docampo R, Bakalara N. A vacuolar-type H+-pyrophosphatase governs maintenance of functional acidocalcisomes and growth of the insect and mammalian forms of Trypanosoma brucei. J Biol Chem 2002;277:37369–37376. [PubMed: 12121996]

Lloyd-Evans E, Morgan AJ, He X, Smith DA, Elliot-Smith E, Sillence DJ, Churchill GC, Schuchman EH, Galione A, Platt FM. Niemann-Pick disease type C1 is a sphingosine storage disease that causes deregulation of lysosomal calcium. Nat Med 2008;14:1247–1255. [PubMed: 18953351]

Lovett JL, Sibley LD. Intracellular calcium stores in Toxoplasma gondii govern invasion of host cells. J Cell Sci 2003;116:3009–3016. [PubMed: 12783987]

Luo S, Ruiz FA, Moreno SN. The acidocalcisome Ca2+-ATPase (TgA1) of Toxoplasma gondii is required for polyphosphate storage, intracellular calcium homeostasis and virulence. Mol Microbiol 2005;55:1034–1045. [PubMed: 15686552]

Luo S, Vieira M, Graves J, Zhong L, Moreno SN. A plasma membrane-type Ca(2+)-ATPase co-localizes with a vacuolar H(+)-pyrophosphatase to acidocalcisomes of Toxoplasma gondii. Embo J 2001;20:55–64. [PubMed: 11226155]

Maddy AH. A critical evaluation of the analysis of membrane proteins by polyacrylamide gel electrophoresis in the presence of dodecyl sulphate. J Theor Biol 1976;62:315–326. [PubMed: 994526]

Maeshima M. TONOPLAST TRANSPORTERS: Organization and Function. Annu Rev Plant Physiol Plant Mol Biol 2001;52:469–497. [PubMed: 11337406]

Martinoia E, Maeshima M, Neuhaus HE. Vacuolar transporters and their essential role in plant metabolism. J Exp Bot 2007;58:83–102. [PubMed: 17110589]

Marty F. Plant vacuoles. Plant Cell 1999;11:587–600. [PubMed: 10213780]

Moreno SN, Zhong L. Acidocalcisomes in Toxoplasma gondii tachyzoites. Biochem J 1996;313(Pt 2): 655–659. [PubMed: 8573106]

Moreno SN, Zhong L, Lu HG, Souza WD, Benchimol M. Vacuolar-type H+-ATPase regulates cytoplasmic pH in Toxoplasma gondii tachyzoites. Biochem J 1998;330(Pt 2):853–860. [PubMed: 9480901]

Moyle J, Mitchell R, Mitchell P. Proton-translocating pyrophosphatase of Rhodospirillum rubrum. FEBS Lett 1972;23:233–236. [PubMed: 4343931]

Muntz K. Protein dynamics and proteolysis in plant vacuoles. J Exp Bot 2007;58:2391–2407. [PubMed: 17545219]

Niemietz CM, Tyerman SD. New potent inhibitors of aquaporins: silver and gold compounds inhibit aquaporins of plant and human origin. FEBS Lett 2002;531:443–447. [PubMed: 12435590]

Olbrich A, Hillmer S, Hinz G, Oliviusson P, Robinson DG. Newly formed vacuoles in root meristems of barley and pea seedlings have characteristics of both protein storage and lytic vacuoles. Plant Physiol 2007;145:1383–1394. [PubMed: 17965174]

Paris N, Stanley CM, Jones RL, Rogers JC. Plant cells contain two functionally distinct vacuolar compartments. Cell 1996;85:563–572. [PubMed: 8653791]

Parussini F, Coppens I, Shah PP, Diamond SL, Carruthers VB. Cathepsin L occupies a vacuolar compartment and is a protein maturase within the endo/exocytic system of *Toxoplasma gondii*. Mol Microbiol. 2010 inpress.

Patel S, Docampo R. Acidic calcium stores open for business: expanding the potential for intracellular Ca(2+) signaling. Trends Cell Biol 20:277–286. [PubMed: 20303271]

Pavlovic-Djuranovic S, Schultz JE, Beitz E. A single aquaporin gene encodes a water/glycerol/urea facilitator in Toxoplasma gondii with similarity to plant tonoplast intrinsic proteins. FEBS Lett 2003;555:500–504. [PubMed: 14675763]

Que X, Ngo H, Lawton J, Gray M, Liu Q, Engel J, Brinen L, Ghosh P, Joiner KA, Reed SL. The cathepsin B of Toxoplasma gondii, toxopain-1, is critical for parasite invasion and rhoptry protein processing. J Biol Chem 2002;277:25791–25797. [PubMed: 12000756]

Rea PA, Kim Y, Sarafian V, Poole RJ, Davies JM, Sanders D. Vacuolar H(+)-translocating pyrophosphatases: a new category of ion translocase. Trends Biochem Sci 1992;17:348–353. [PubMed: 1329278]

Rea PA, Poole RJ. Chromatographic Resolution of H-Translocating Pyrophosphatase from H-Translocating ATPase of Higher Plant Tonoplast. Plant Physiol 1986;81:126–129. [PubMed: 16664761]

Robibaro B, Stedman TT, Coppens I, Ngo HM, Pypaert M, Bivona T, Nam HW, Joiner KA. Toxoplasma gondii Rab5 enhances cholesterol acquisition from host cells. Cell Microbiol 2002;4:139–152. [PubMed: 11906451]

Rodrigues CO, Ruiz FA, Rohloff P, Scott DA, Moreno SN. Characterization of isolated acidocalcisomes from Toxoplasma gondii tachyzoites reveals a novel pool of hydrolyzable polyphosphate. J Biol Chem 2002;277:48650–48656. [PubMed: 12379647]

Rodrigues CO, Scott DA, Bailey BN, De Souza W, Benchimol M, Moreno B, Urbina JA, Oldfield E, Moreno SN. Vacuolar proton pyrophosphatase activity and pyrophosphate (PPi) in Toxoplasma gondii as possible chemotherapeutic targets. Biochem J 2000;349(Pt 3):737–745. [PubMed: 10903134]

Rodrigues CO, Scott DA, Docampo R. Presence of a vacuolar H+-pyrophosphatase in promastigotes of Leishmania donovani and its localization to a different compartment from the vacuolar H+-ATPase. Biochem J 1999;340(Pt 3):759–766. [PubMed: 10359662]

Rogers JC, Dean D, Heck GR. Aleurain: a barley thiol protease closely related to mammalian cathepsin H. Proc Natl Acad Sci U S A 1985;82:6512–6516. [PubMed: 3901004]

Rohloff P, Montalvetti A, Docampo R. Acidocalcisomes and the contractile vacuole complex are involved in osmoregulation in Trypanosoma cruzi. J Biol Chem 2004;279:52270–52281. [PubMed: 15466463]

Roos DS, Donald RG, Morrissette NS, Moulton AL. Molecular tools for genetic dissection of the protozoan parasite Toxoplasma gondii. Methods Cell Biol 1994;45:27–63. [PubMed: 7707991]

Sarafian V, Kim Y, Poole RJ, Rea PA. Molecular cloning and sequence of cDNA encoding the pyrophosphate-energized vacuolar membrane proton pump of Arabidopsis thaliana. Proc Natl Acad Sci U S A 1992;89:1775–1779. [PubMed: 1311852]

Scott DA, de Souza W, Benchimol M, Zhong L, Lu HG, Moreno SN, Docampo R. Presence of a plant-like proton-pumping pyrophosphatase in acidocalcisomes of Trypanosoma cruzi. J Biol Chem 1998;273:22151–22158. [PubMed: 9705361]

Shaw MK, Roos DS, Tilney LG. Acidic compartments and rhoptry formation in Toxoplasma gondii. Parasitology 1998;117(Pt 5):435–443. [PubMed: 9836308]

Stenmark H, Olkkonen VM. The Rab GTPase family. Genome Biol 2001;2 REVIEWS3007.

Striepen B, He CY, Matrajt M, Soldati D, Roos DS. Expression, selection, and organellar targeting of the green fluorescent protein in Toxoplasma gondii. Mol Biochem Parasitol 1998;92:325–338. [PubMed: 9657336]

Takamori S, Holt M, Stenius K, Lemke EA, Gronborg M, Riedel D, Urlaub H, Schenck S, Brugger B, Ringler P, Muller SA, Rammner B, Grater F, Hub JS, De Groot BL, Mieskes G, Moriyama Y, Klingauf J, Grubmuller H, Heuser J, Wieland F, Jahn R. Molecular anatomy of a trafficking organelle. Cell 2006;127:831–846. [PubMed: 17110340]

Tardieux I, Menard R. Migration of Apicomplexa across biological barriers: the Toxoplasma and Plasmodium rides. Traffic 2008;9:627–635. [PubMed: 18194412]

Vincent JL, Brewin NJ. Immunolocalization of a cysteine protease in vacuoles, vesicles, and symbiosomes of pea nodule cells. Plant Physiol 2000;123:521–530. [PubMed: 10859182]

Zeuthen T, Wu B, Pavlovic-Djuranovic S, Holm LM, Uzcategui NL, Duszenko M, Kun JF, Schultz JE, Beitz E. Ammonia permeability of the aquaglyceroporins from Plasmodium falciparum,

Toxoplasma gondii and Trypansoma brucei. Mol Microbiol 2006;61:1598–1608. [PubMed: 16889642]

Zhen RG, Baykov AA, Bakuleva NP, Rea PA. Aminomethylenediphosphonate: A Potent Type-Specific Inhibitor of Both Plant and Phototrophic Bacterial H+-Pyrophosphatases. Plant Physiol 1994;104:153–159. [PubMed: 12232069]

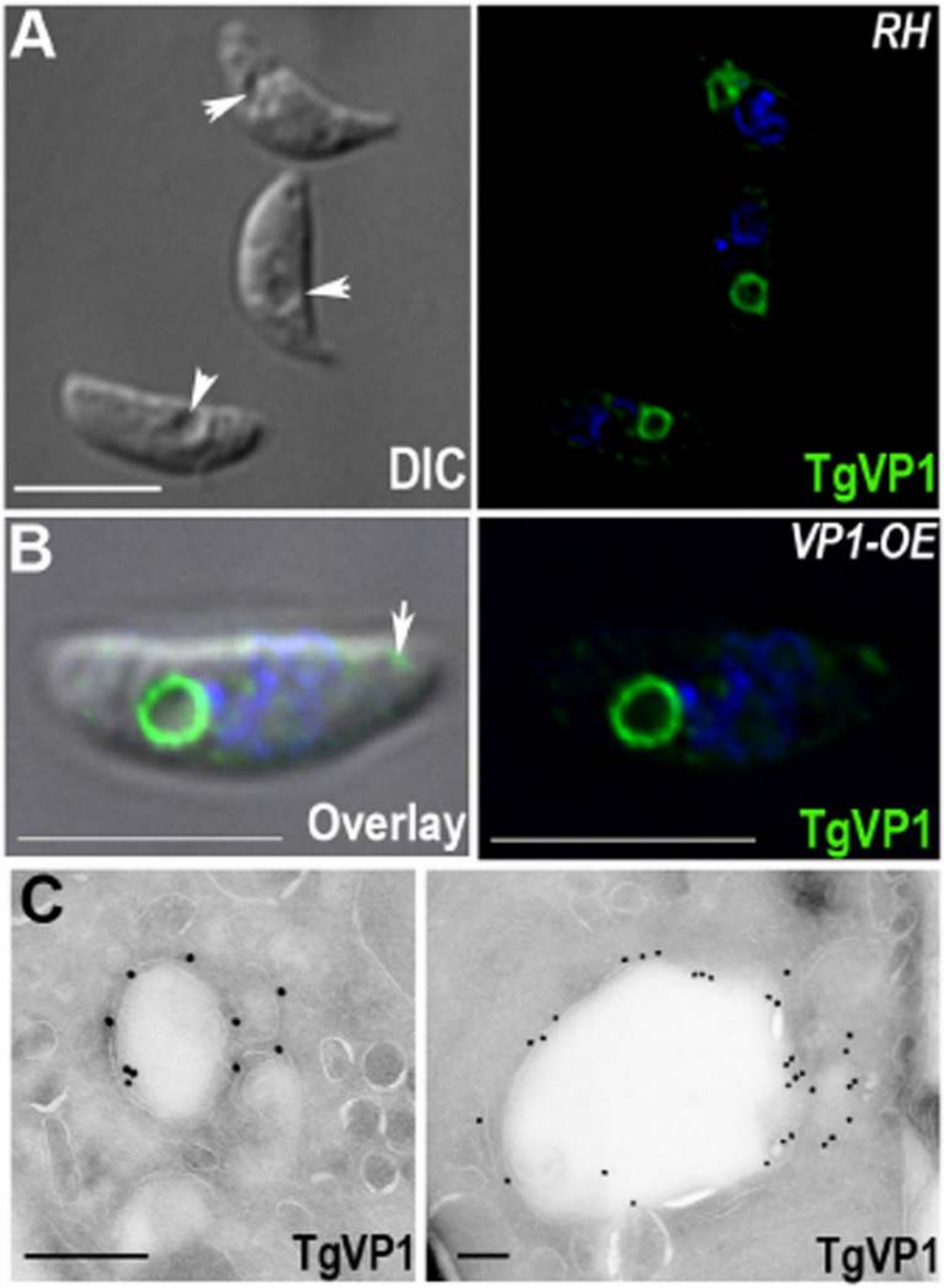

Fig. 1.

Antibody specific to the vacuolar proton pyrophosphatase (TgVP1) consistently labels a vacuolar structure in extracellular tachyzoites. (**A**) Extracellular tachyzoites were incubated in Ringer's buffer, fixed and stained with anti-TgVP1 antibody (1:4,000) and DAPI (*blue*). *Left panel* shows the DIC images of three parasites with *arrows* pointing at a large vacuolar compartment clearly visible. The *right panel* shows strong labeling with anti-TgVP1 in a large vacuole in the three parasites. (**B**) Reaction with anti-TgVP1 in tachyzoites overexpressing TgVP1 (TgVP1-OE) (arrow point to an acidocalcisome). (**C**) Immunogold electron microscopy labeling with anti-TgVP1 antibody of a small empty vacuole with the size of an acidocalcisome (*left*) and a large vacuolar compartment (*right*). The antibody used

was the purified rabbit anti-serum generated against the peptide: SGKNEYGMSEDDPRN. Bars A, B = 5 μm, D: 200 nm

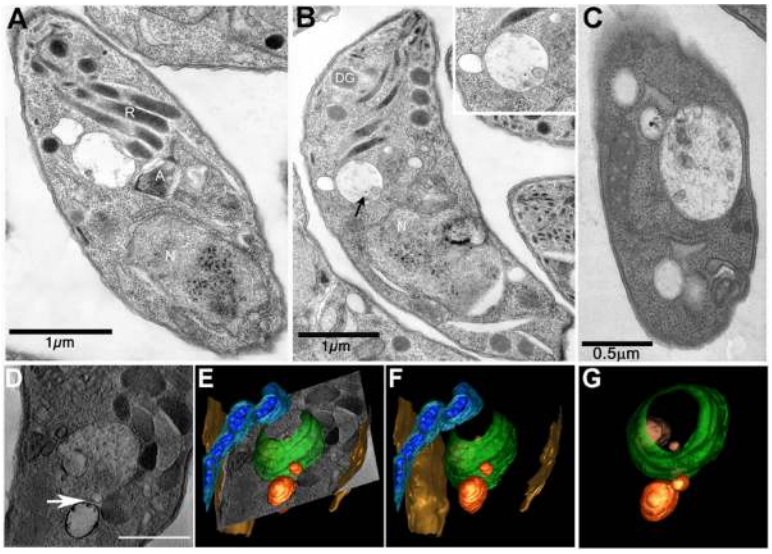

Fig. 2.

Transmission electron microscopy of recently released tachyzoites. (**A–C**) Thin sections of whole tachyzoites showing a large vacuole. Arrow in (**B**) points to an acidocalcisome-like organelle. The inset shows the enlargement of the vacuole containing this structure. The presence of internal vesicles is also evident inside the large vacuole in (**C**). R: rhoptry; DG: dense granule; N: nucleus; A: apicoplast. Scale bars: A, B = 1 μm; C = 0.5 μm. (**D–G**) 3D reconstruction of a *T. gondii* tachyzoite by electron tomography. The image in **D** shows a profile of a tachyzoite within the reconstructed volume showing intracellular structures, an acidocalcisome, and a large vacuole containing internal vesicles. The 3D models (**E–G**) show a segmented plasma membrane (*golden yellow*), the mitochondrion (*light blue*), acidocalcisomes (*orange*) and a large vacuole (*green*). Different tilted views of the models are presented where it is possible to observe internal vesicles (*dark gold*). *Arrow* in **D** shows point of contact of an acidocalcisome with the large vacuole.

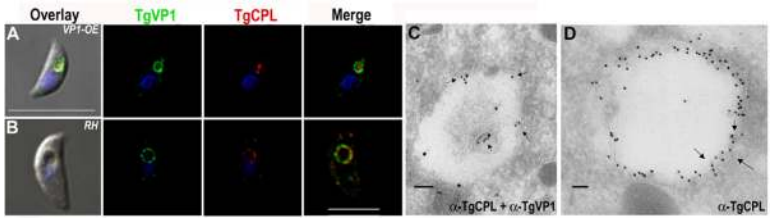

Fig. 3.

Co-localization of TgVP1 and TgCPL as observed by IFA and immunogold electron microscopy. Tachyzoites were fixed and stained with rabbit anti-TgVP1 antibody (1:4,000) (*green*), and mouse anti-CPL antibody (1:400) (*red*), and DAPI (*blue*). Both antibodies localize to the same compartment (*merge* and *overlay*). Anti-TgVP1 labels the membrane of a large vacuole (*green* and *merge in* (**A**) and (**B**)). Anti-TgCPL is also observed at the membrane of the large vacuole (*red* and *merge in* (**B**)). Scale bars: A = 10 μm; B = 3 μm. (**C**) Immunogold electron microscopy showing co-localization of TgVP1 (rabbit serum) with TgCPL. Co-localization of TgVP1 (5 nm gold particles, *arrows*) with TgCPL (10 nm gold particles) to the membrane of a large vacuole (**C**, **D**) or to internal vesicles (**C**). Scale bars = 0.1 μm.

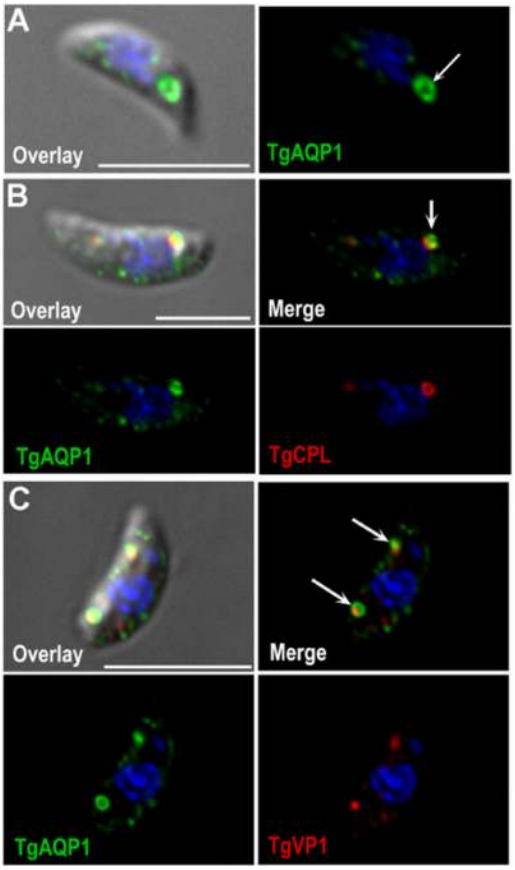

Fig. 4.

Localization of *T. gondii* aquaporin-1 (TgAQP1) in extracellular tachyzoites to a large vacuolar structure. To help ascertain the correct location of TgAQP1, tachyzoites over-expressing the native version of TgAQP1 were used. Detection of TgAQP1 was performed using an affinity purified antibody against the C-terminal region of TgAQP1 (1:200). (**A**) Localization of TgAQP1 to a large vacuole, evident by DIC overlay and IFA (*arrow*). (**B**) Co-localization of TgAQP1 (*green*) with endogenous TgCPL (*red*). Arrow in merge shows co-localization (*yellow*) of TgAQP1 (*green*) with TgCPL (*red*). (**C**) Co-localization of TgAQP1 (*green*) with endogenous TgVP1 (*red*). Bottom arrow in merge shows a vacuole and localization of TgVP1 (guinea pig anti-serum at 1:100) where TgAQP1 is located. Top arrow shows co-localization of TgAQP1 and TgVP1 in a second vacuole or putative acidocalcisome. Scale bars: A = 5 μm, B: 3 μm and C = 5 μm.

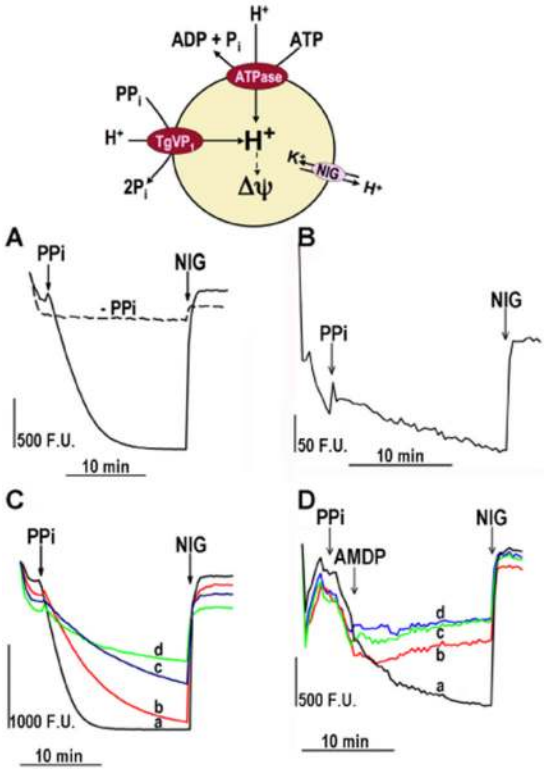

Fig. 5.

PP_i-driven proton transport in PLV-enriched fractions. Acridine orange accumulates in an acidic compartment and the quenching of the fluorescence correlates with the ΔpH (inside acidic). This accumulation is strictly dependent on the presence of PP_i indicating a pyrophosphatase activity. The slope of the tracings correlates with the activity of the enzyme. This uptake is reverted upon addition of nigericin, a K^+/H^+ ionophore due to protons being released from the vesicular compartment. PLV-enriched fraction (0.15 μg protein/ml) was added to a buffer containing 130 mM KCl, 2 mM potassium phosphate, 2 mM $MgCl_2$, 10 mM Hepes, pH 7.2, and 3 μM acridine orange. PP_i (0.1 mM), ATP (0.5 mM), and nigericin (0.5 μM) were added where indicated. (A, C, and D) **(A)** Activity of fractions obtained from TgVP1-OE cells. (**B**) Activity of fractions obtained from RH cells. (**C**) Effect of buffer composition on the PP_i-stimulated proton transport. The buffer described above was supplemented with either 130 mM KCl (*trace a*), 65 mM KCl and 130 mM sucrose (*trace b*); 130 mM NaCl (*trace c*) or 250 mM sucrose (*trace d*). (**D**) Inhibitory effect by AMDP (*trace a*: 0; *trace b*: 40 μM, *trace c*: 100 μM; *trace d*: 500 μM). F.U. indicates arbitrary fluorescence units.

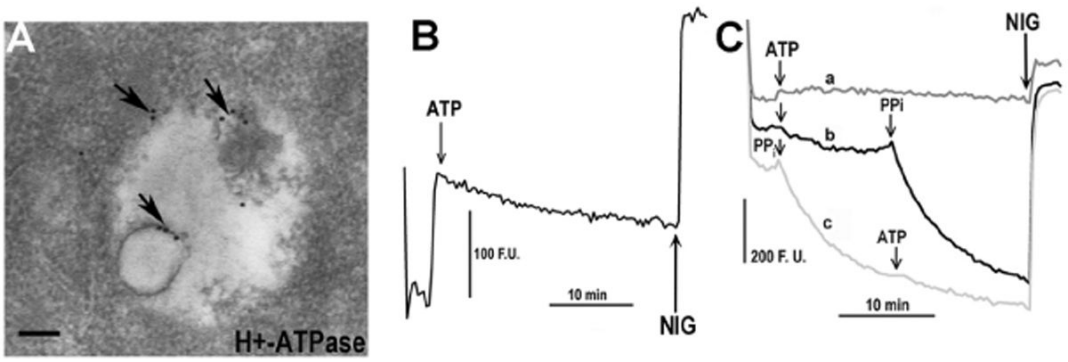

Fig. 6.

Localization of V-H^+-ATPase in the PLV. **(A)** Immunogold electron microscopy showing labeling of the large vacuole and internal vesicles with a rabbit polyclonal antibody against *D. discoideum* V-H^+-ATPase (Moreno et al., 1998) (10 nm gold particles). Bar = 0.1 μm. (**B**) ATP-driven H^+ transport in PLV-enriched fractions from wild type parasites. **(C)** Proton transport in PLV-enriched fractions from TgVP1-OE parasites stimulated by ATP (traces a and b) in the presence of bafilomycin (trace a). Addition of PP_i after ATP shows a significant increase in proton transport. Trace c shows first the transport stimulated by PP_i and addition of ATP does not affect the rate when added subsequently. All incubations were done with PLV fraction (0.15 μg protein/ml) in the same buffer described in the legend for Fig. 5A and ATP (1 mM), PP_i (0.1 mM) and nigericin (0.5 μM) were added where indicated. F.U. indicates arbitrary fluorescence units.

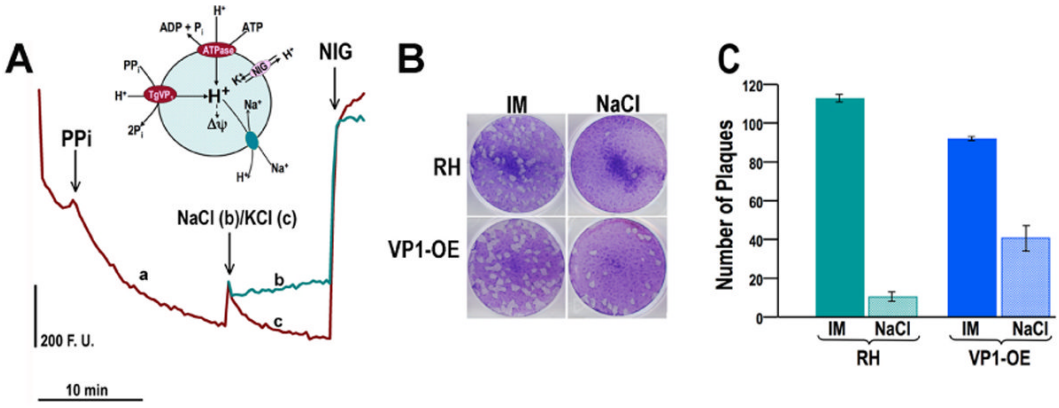

Fig. 7.

TgVP1-overexpressing cells are more resistant to salt stress and evidence for a Na^+/H^+ exchanger. (**A**) Upon addition of sodium, acridine orange is released from the vacuolar compartment due to alkalynization. This is because there is an exchange of sodium for protons strongly suggesting the operation of a sodium proton exchanger (see scheme). Effect of 80 mM NaCl (*trace b*) or 80 mM KCl (*trace c*) addition. F.U. arbitrary fluorescence units at 470–526 nm. Other conditions as in Fig. 5A. (**B**) Plaque assays comparing growth of RH vs. TgVP1-OE cells pre-incubated for 30 min in invasion media (IM) or PBS containing additional 150 mM NaCl (NaCl) (287 mM in total). (**C**) Plaque number was quantified in four independent wells for each condition. Bars represent standard errors.

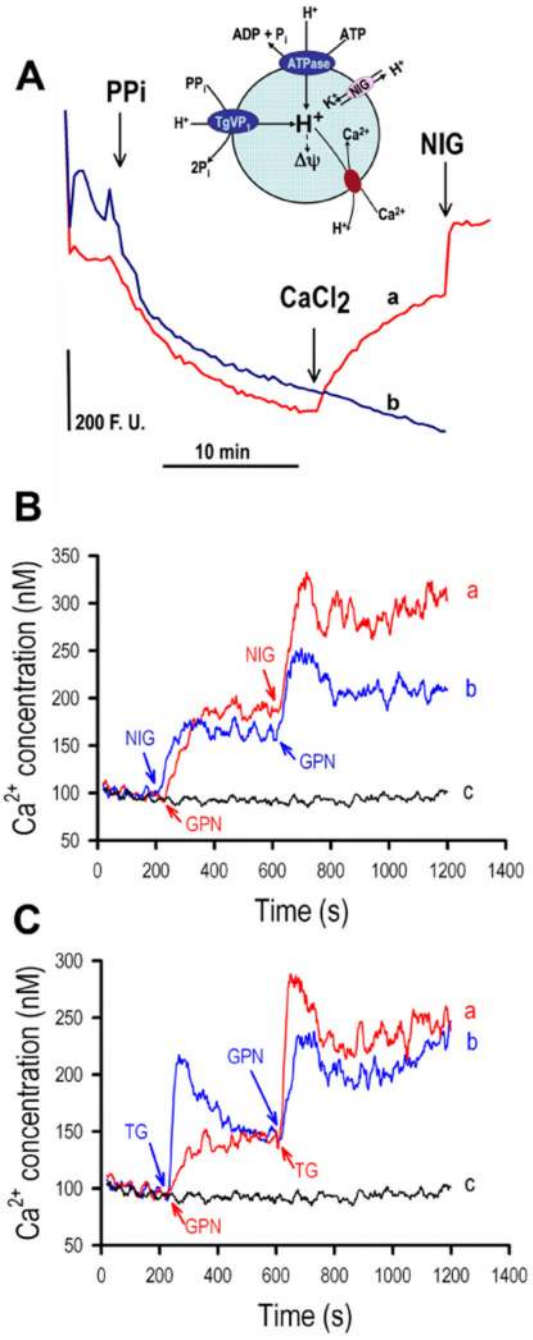

Fig. 8.

The PLV contains calcium, which can be released by GPN. (**A**) Biochemical evidence of a calcium-proton exchange mechanism in tachyzoites. Upon addition of calcium (100 mM, trace a) to a previously PP_i-energized PLV fraction, a discernable release of protons is evident that was not observed in the control experiment (see scheme for proposed scenario). Other conditions as in Fig. 5A. (**B** and **C**) Effect to GPN on intracellular calcium levels. *T. gondii* tachyzoites were loaded with fura 2-AM and cytosolic calcium concentration was monitored in BAG containing 1 mM EGTA at a 2×10^7 cells/ml final concentration in a cuvette and scanned in a Hitachi F-4500 spectrofluorometer. (B) Cytosolic calcium concentration upon sequential addition of GPN followed by nigericin (NIG) (*trace a*). *Trace*

b shows a similar response when the order of addition is reversed with GPN addition after the addition of NIG. Baseline calcium concentration with no additions is shown in *trace c*. (**C**) Cytosolic calcium concentration upon sequential addition of GPN and thapsigargin (TG) (trace a). *Trace b* shows a similar response when the order of addition is reversed with TG addition followed by GPN. Final concentration of agonists were: GPN, 20 μM; thapsigargin, 2 μM; nigericin, 1 μM.

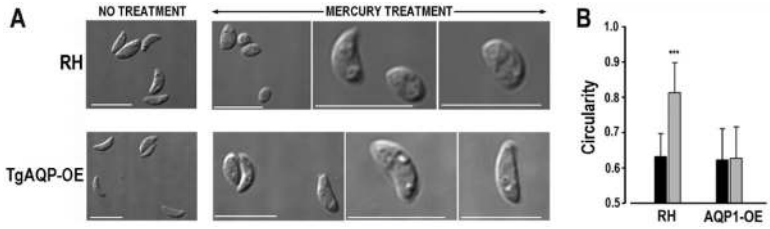

Fig. 9.

Response to $HgCl_2$ in TgAQP1 overexpressing extracellular tachyzoites. Extracellular tachyzoites were collected, removed from culture media, and resuspended in buffer A with glucose (BAG). (A) RH and TgAQP1 overexpressing tachyzoites were either kept in BAG for 5 min (`no treatment') or incubated in BAG with $HgCl_2$ at a final concentration of 1 μM for 5 min (`mercury treatment'). Cells were then fixed with paraformaldehyde for 1 hour and mounted on coverslips for visualization using DIC microscopy. Scale bars for A = 10 μm. (**B**) Morphometric analysis of RH and TgAQP1 overexpressing cells in the absence (black bars) or presence (gray bars) of 1 μM $HgCl_2$. Circularity measurements were made on 50 randomly chosen parasites for each treatment. Error bars are standard deviation, *** $P<0.001$.

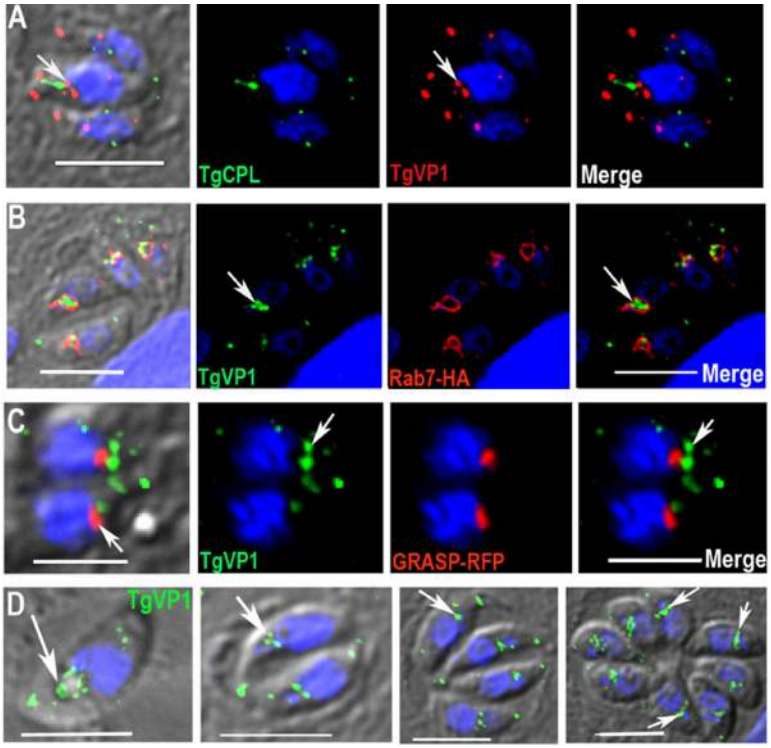

Fig. 10.

The PLV fragments after host cell invasion. (**A**) Lack of co-localization of anti-TgCPL used at a dilution of 1:400 (*green*) and anti-TgVP1 used at a dilution of 1:4,000 (*red*). The *arrows* indicate a typical appearance of vesicles labeled with anti-TgVP1 apical to the nucleus. hTert monolayers were infected with 1.5×10^6 tachyzoites and fixed 20 hours later for IFA assay. (**B**) Co-localization of anti-TgVP1 (*green*) and antibodies against the HA tag of TgRab7 used at a dilution of 1:800 (*red*). The arrows points at vesicles labeled with the anti-TgVP1 antibody. (**C**) Labeling by anti-TgVP1 is in a post-Golgi compartment. Parasites were transfected with the plasmid pTubGRASP55-RFP/sagCAT. The red labeling comes from the direct fluorescence of the red fluorescent protein (arrow points at the red-labeled compartment in left panel). The labeling of vesicles with anti-TgVP1 is indicated by arrows in the TgVP1 and Merge panels. (**D**) Replicating, intracellular parasites were labeled at different stages of division with anti-TgVP1 antibodies. The arrows show the appearance of the PLV as the cells divide. Anti-TgVP1 primary antibody was used at 1:4,000 and goat anti-rabbit Alexa488 as secondary antibody was at 1:1000. Blue fluorescence = DAPI. Scale bars =5 μm.

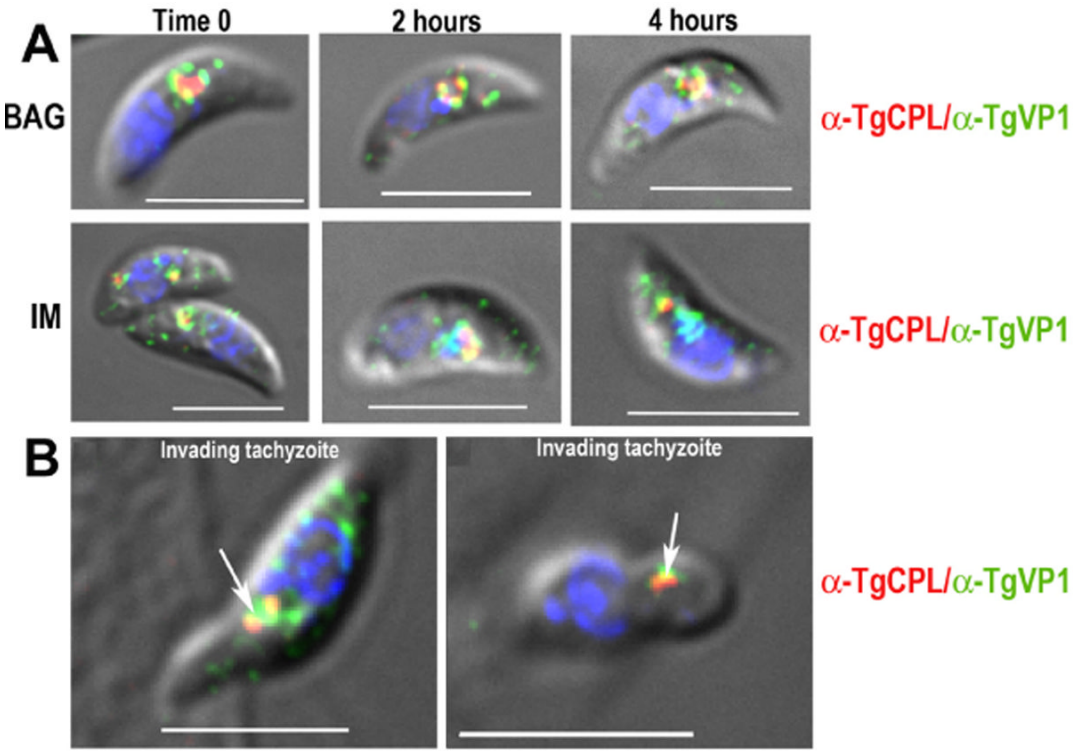

Fig. 11.

The PLV is evident in extracellular parasites soon after release from host cells. (**A**) Intracellular tachyzoites were obtained after scrapping off infected host monolayers and fixed immediately (time 0), or incubated for 2 and 4 hours in BAG or IM. Anti-TgCPL and anti-TgVP1 antibodies were used to visualize the PLVs at those times. The most common phenotype is shown. Table 2 shows the quantification of these cells. (**B**) Tachyzoites were allowed to invade hTert monolayers for 5 min at 37 °C after a pre-incubation of 15 min on ice. Cells were immediately fixed and anti-TgCPL and anti-TgVP1 antibodies were used to visualize the PLV. Antibody concentrations are indicated in the legend for Fig. 3. Scale Bars = 5 μm.

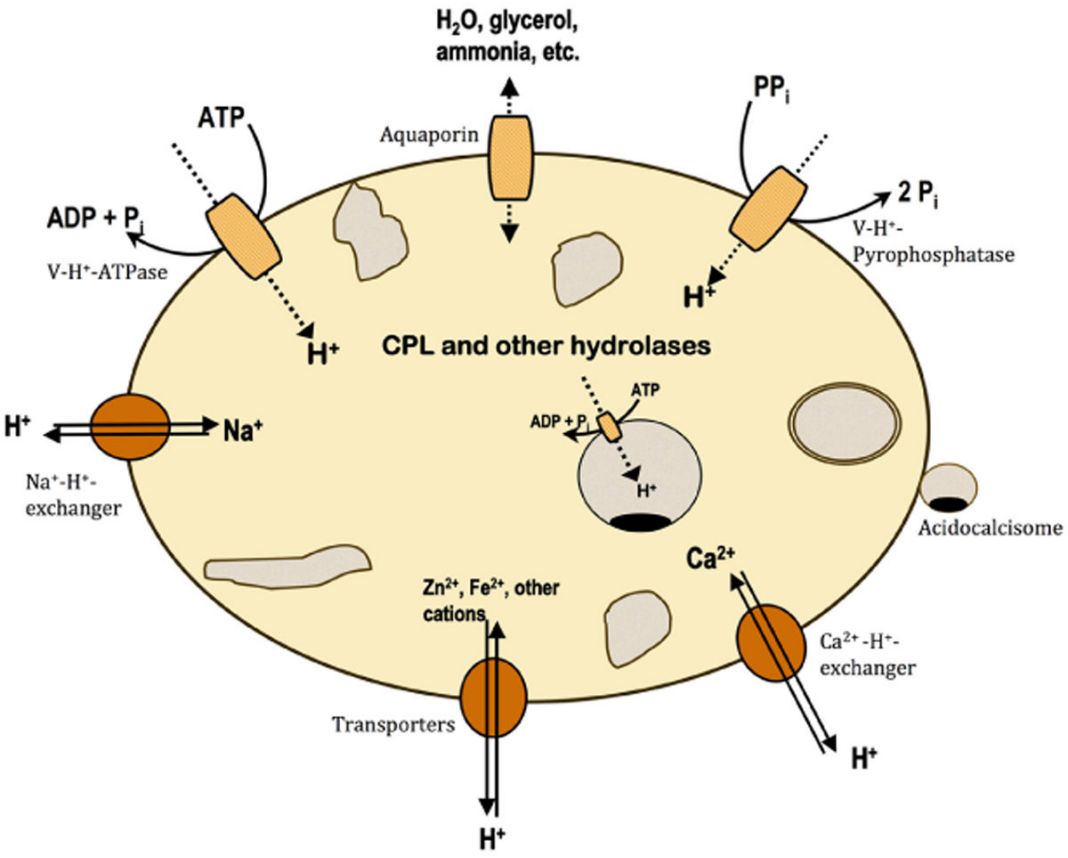

Fig. 12.

Schematic representation of the plant-like vacuole. The H^+ gradient is established by a vacuolar H^+-ATPase (V-H^+-ATPase) and a vacuolar proton pyrophosphatase (V-H^+-PPase). An aquaporin channel would transport water or other osmolytes which could help the parasite deal with environmental stress. Other potential transporters include Na^+/H^+, and Ca^{2+}/H^+ exchangers. As in the plant vacuole, other transporters may be present which could transport other cations using the proton gradient generated by the proton pumps. Some internal vesicles and acidocalcisomes are also shown.

Table 1

Enrichment of Fraction 1 in AMDP-sensitive PPase activity.

Enzyme	Parasites	P3	Fraction 1[a]
V-H$^+$-Ppase[b] (nmol/min/mg)	RH	2.27 ± 0.24	45.77 ± 4.51
	OE	19.32 ± 0.17	225.08 ± 3.85
Acid phosphatase[c] (nmol/min/mg)	RH	32.60 ± 0.55	55.25 ± 1.27
	OE	12.64 ± 0.12	105.05 ± 2.60
Soluble PPase[c] (nmol/min/mg)	RH	14.00 ± 0.77	11.38 ± 0.10
	OE	14.27 ± 0.50	37.83 ± 1.72

Comparison of the values for columns P3 (Pellet 3 from fractionation schematic in Fig. S4) and Fraction 1 show a significant increase in the activities for the PLV markers (V-H$^+$-PPase and acid phosphatase) and not in the activity of the soluble PPase (a cytosolic enzyme) in RH tachyzoites. The activity of the V-H$^+$-PPase is higher in the fraction obtained from the TgPPase-OE (OE) cells than in the fraction from RH tachyzoites.

These results are representative of more than 10 fractionation experiments.

[a] Fraction 1 was obtained through subcellular fractionation of *T. gondii* tachyzoites following the steps described in the supplementary Fig. S4.

[b] This activity is the AMDP-sensitive pyrophosphate hydrolysis activity measured as explained under Experimental Procedures.

[c] Protocols for the determination of these enzyme activities are explained under Experimental Procedures.

TABLE 2

Number of open vs. closed PLVs in recently released tachyzoites.

Conditions	Total Number of Parasites[a]	Number of Open Vacuoles[b]	Number of Closed Vacuoles
BAG	38	26 (68%)	3 (7%)
IM	35	7 (24%)	23 (67%)

The results presented are from one experiment out of 3. The other two experiments gave similar results.

Tachyzoites, were collected by scrapping off the host monolayer and releasing parasites by passing them through a 25 G syringe needle. Cells were collected in either BAG or IM and the numbers in the table are the ones obtained immediately after isolating the parasites (Time 0 in Fig. 11). Vacuoles were considered open when their diameter was larger than 0.5 μm. Vacuoles were considered closed when their diameter was equal or smaller than 0.5 μm.

[a]These numbers are the average number of parasites counted in 5 different fields. Parasites with visible vacuoles by DIC and labeled with anti-TgVP1 were counted. Total cells evaluated were 189 in BAG and 177 in IM.

[b]Numbers given in parentheses represent the percentage of cells in open or closed configuration. Cells with no clear PLV were not counted as either open or closed, and represented less than 25% of the total population.